INTERNATIONAL STANDARD

ISO 27852

Second edition
2016-07-01

Space systems — Estimation of orbit lifetime

Systèmes spatiaux — Estimation de la durée de vie en orbite

Reference number
ISO 27852:2016(E)

ISO copyright office
Ch. de Blandonnet 8 • CP 401
CH-1214 Vernier, Geneva, Switzerland
Tel. +41 22 749 01 11
Fax +41 22 749 09 47
copyright@iso.org
www.iso.org

Contents

Page

Foreword

ISO (the International Organization for Standardization) is a worldwide federation of national standards bodies (ISO member bodies). The work of preparing International Standards is normally carried out through ISO technical committees. Each member body interested in a subject for which a technical committee has been established has the right to be represented on that committee. International organizations, governmental and non-governmental, in liaison with ISO, also take part in the work. ISO collaborates closely with the International Electrotechnical Commission (IEC) on all matters of electrotechnical standardization.

The procedures used to develop this document and those intended for its further maintenance are described in the ISO/IEC Directives, Part 1. In particular the different approval criteria needed for the different types of ISO documents should be noted. This document was drafted in accordance with the editorial rules of the ISO/IEC Directives, Part 2 (see www.iso.org/directives).

Attention is drawn to the possibility that some of the elements of this document may be the subject of patent rights. ISO shall not be held responsible for identifying any or all such patent rights. Details of any patent rights identified during the development of the document will be in the Introduction and/or on the ISO list of patent declarations received (see www.iso.org/patents).

Any trade name used in this document is information given for the convenience of users and does not constitute an endorsement.

For an explanation on the meaning of ISO specific terms and expressions related to conformity assessment, as well as information about ISO's adherence to the WTO principles in the Technical Barriers to Trade (TBT) see the following URL: Foreword - Supplementary information

The committee responsible for this document is ISO/TC 20, *Aircraft and space vehicles*, Subcommittee SC 14, *Space systems and operations*.

This second edition cancels and replaces the first edition (ISO 27852:2011), which has been technically revised.

Introduction

This International Standard is a supporting document to ISO 24113 and the GEO and LEO disposal standards that are derived from ISO 24113. The purpose of this International Standard is to provide a common consensus approach to determining orbit lifetime, one that is sufficiently precise and easily implemented for the purpose of demonstrating compliance with ISO 24113. This project offers standardized guidance and analysis methods to estimate orbital lifetime for all LEO-crossing orbit classes.

Space systems — Estimation of orbit lifetime

1 Scope

This International Standard describes a process for the estimation of orbit lifetime for spacecraft, launch vehicles, upper stages and associated debris in LEO-crossing orbits.

This International Standard also clarifies the following:

a) modelling approaches and resources for solar and geomagnetic activity modelling;

b) resources for atmosphere model selection;

c) approaches for spacecraft ballistic coefficient estimation.

2 Normative References

The following documents, in whole or in part, are normatively referenced in this document and are indispensable for its application. For dated references, only the edition cited applies. For undated references, the latest edition of the referenced document (including any amendments) applies.

ISO 24113, *Space systems — Space debris mitigation requirements*

3 Terms, definitions, symbols and abbreviated terms

3.1 Terms and definitions

For the purposes of this document, the terms and definitions given in ISO 24113 and the following apply.

3.1.1
orbit lifetime
elapsed time between the orbiting spacecraft's initial or reference position and orbit demise/reentry

Note 1 to entry: An example of the orbiting spacecraft's reference position is the post-mission orbit.

Note 2 to entry: The orbit's decay is typically represented by the reduction in perigee and apogee altitudes (or radii) as shown in Figure 1.

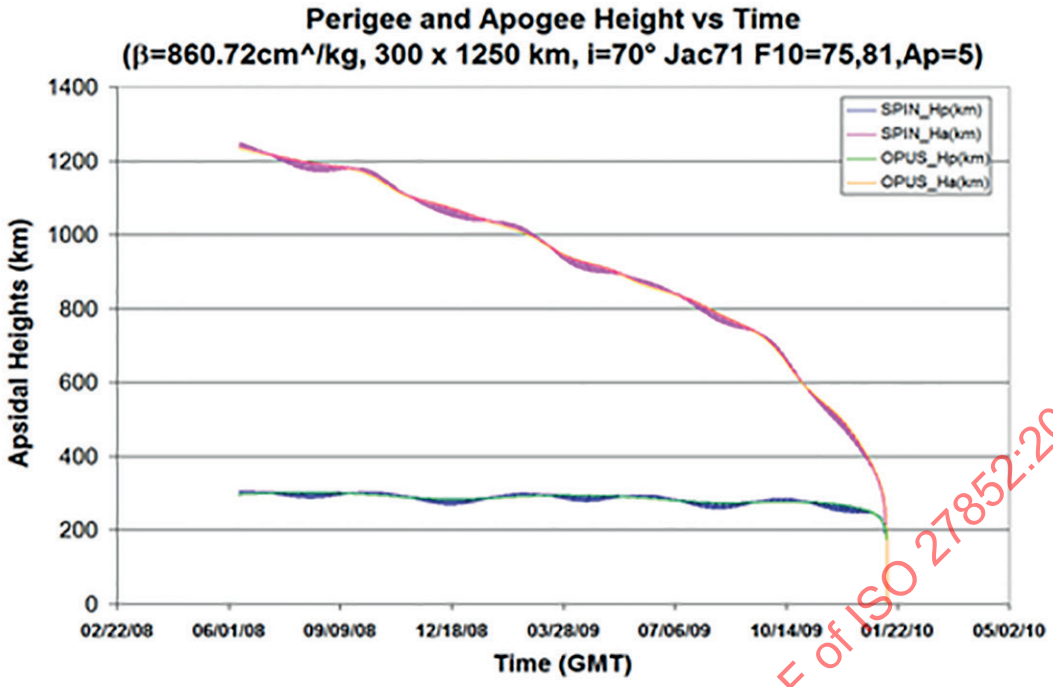

Figure 1 — Sample of orbit lifetime decay profile

3.1.2
earth equatorial radius
equatorial radius of the Earth

Note 1 to entry: The equatorial radius of the Earth is taken as 6 378,137 km and this radius is used as the reference for the Earth's surface from which the orbit regions are defined.

3.1.3
high area-to-mass
HAMR
space objects are considered to be high area-to-mass (or HAMR) objects if the ratio of area to mass exceeds 0,1 m^2/kg

3.1.4
LEO-crossing orbit
low-earth orbit, defined as an orbit with perigee altitude of 2 000 km or less

Note 1 to entry: As can be seen in Figure A.1, orbits having this definition encompass the majority of the high spatial density spike of spacecraft and space debris.

3.1.5
long-duration orbit lifetime prediction
orbit lifetime prediction spanning two solar cycles or more (e.g. 25-year orbit lifetime)

3.1.6
mission phase
period of a mission during which specified communications characteristics are fixed.

Note 1 to entry: The transition between two consecutive mission phases may cause an interruption of the communications services.

3.1.7
post-mission orbit lifetime
duration of the orbit after completion of all mission phases

Note 1 to entry: The disposal phase duration is a component of post-mission duration.

3.1.8
space object
man-made object in outer space

3.1.9
orbit
path followed by a space object

3.1.10
solar cycle
≈11-year solar cycle based on the 13-month running mean for monthly sunspot number and is highly correlated with the 13-month running mean for monthly solar radio flux measurements at the 10,7 cm wavelength

Note 1 to entry: Historical records back to the earliest recorded data (1945) are shown in Figure 2.

Note 2 to entry: For reference, the 25-year post-mission orbit lifetime constraint specified in ISO 24113 is overlaid onto the historical data; it can be seen that multiple solar cycles are encapsulated by this long time duration.

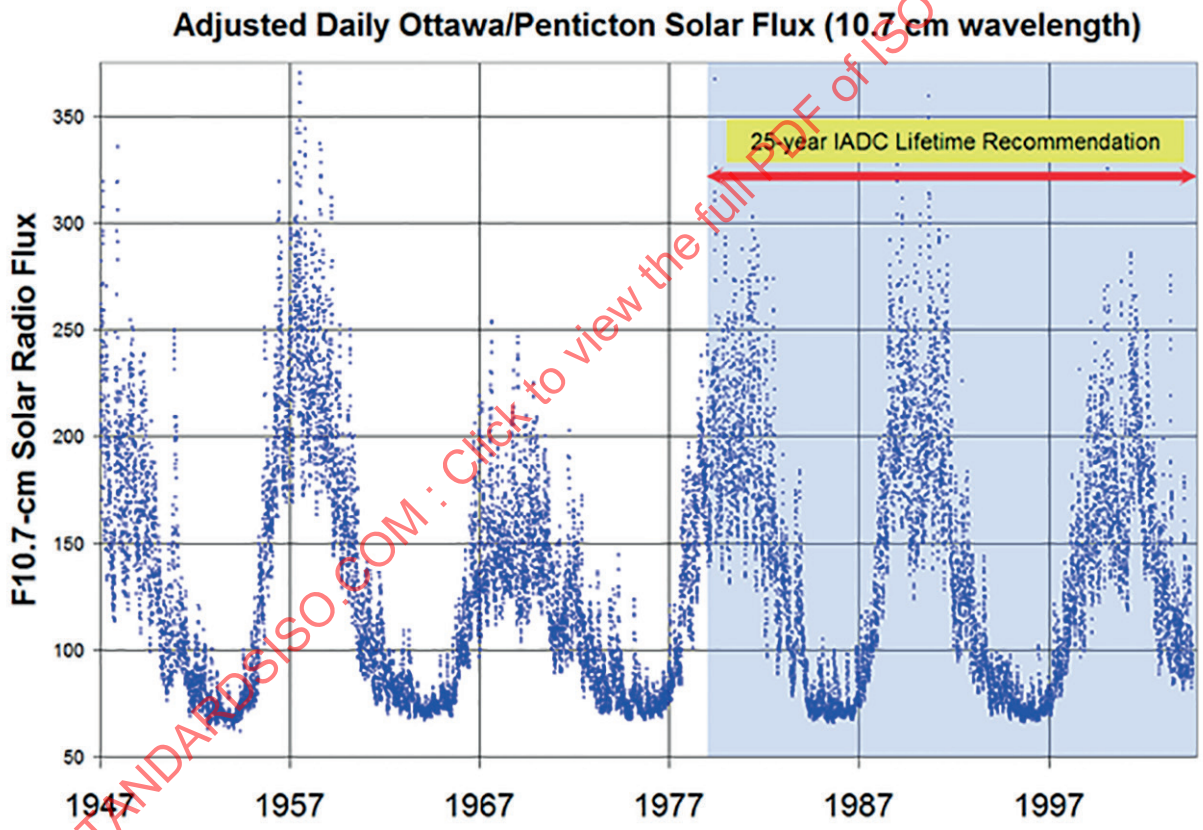

Figure 2 — Solar cycle (≈11-year duration)

3.2 Symbols

a	orbit semi-major axis
A	spacecraft cross-sectional area with respect to the relative wind
A_p	earth daily geomagnetic index
β	ballistic coefficient of spacecraft = $C_D \cdot A/m$
C_D	spacecraft drag coefficient
C_R	spacecraft reflectivity coefficient

e	orbit eccentricity
$F_{10,7}$	solar radio flux observed daily at 2 800 MHz (10,7 cm) in solar flux units (10^{-22}W m^{-2} Hz^{-1})
$F_{10,7}$ Bar	solar radio flux at 2 800 MHz (10,7 cm), averaged over three solar rotations
H_a	apogee altitude = a (1 + e) − R_e
H_p	perigee altitude = a (1 − e) − R_e
m	mass of spacecraft
R_e	equatorial radius of the Earth

3.3 Abbreviated terms

3Bdy	third-body (perturbations)
CAD	computer-aided design
GEO	geosynchronous earth orbit
GTO	geosynchronous transfer orbit
HAMR	high area-to-mass ratio
IADC	Inter-Agency Space Debris Coordination Committee
ISO	International Organization for Standardization
LEO	low earth orbit
N/A	not applicable
RAAN	orbit right ascension of the ascending node (angle between vernal equinox and orbit ascending node, measured CCW in equatorial plane, looking in −Z direction)
SRP	solar radiation pressure
STSC	Scientific and Technical Subcommittee of the Committee
UNCOPUOS	United Nations Committee on the Peaceful Uses of Outer Space

4 Orbit lifetime estimation

4.1 General requirements

The orbital lifetime of LEO-crossing mission-related objects shall be estimated using the processes specified in this International Standard. In addition to any user-imposed constraints, the post-mission portion of the resulting orbit lifetime estimate shall then be constrained to a maximum of 25 years per ISO 24113 using a combination of (a) initial orbit selection, (b) spacecraft vehicle design, (c) spacecraft launch and early orbit concepts of operation which minimize LEO-crossing objects, (d) spacecraft ballistic parameter modifications at EOL, and (e) spacecraft deorbit maneuvers.

4.2 Definition of orbit lifetime estimation process

The orbit lifetime estimation process is represented generically in Figure 3.

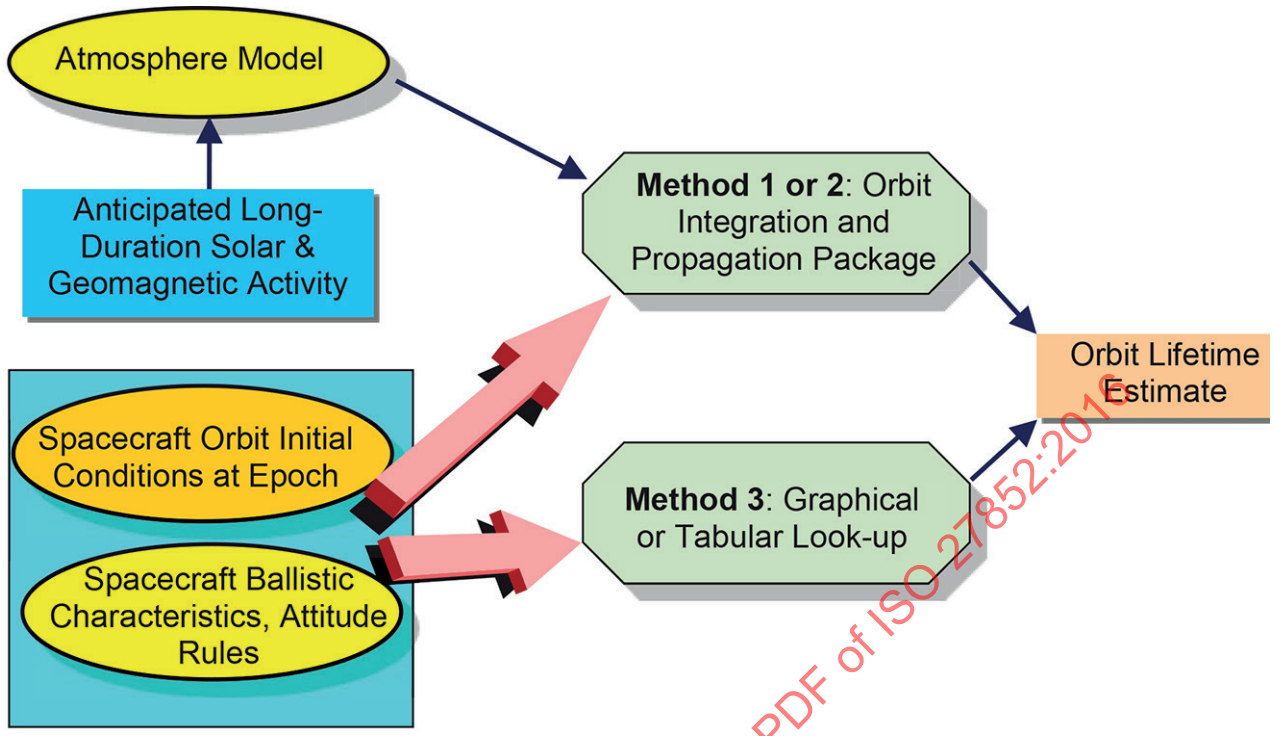

Figure 3 — Orbit lifetime estimation process[4]

5 Orbit lifetime estimation methods and applicability

5.1 General

There are three basic analysis methods used to estimate orbit lifetime,[3] as depicted in Figure 3. Determination of the method used to estimate orbital lifetime for a specific space object shall be based upon the orbit type and perturbations experienced by the spacecraft as shown in Table 1.

Table 1 — Applicable method with mandated conservative margins of error (in percent) and required perturbation modelling

	Special orbit		Conservative margin applied to each method			
Orbit apogee altitude, km	**Sun-sync?**	**High area-to-mass?**	**Method 1: Numerical integration**	**Method 2: Semi-analytic**	**Method 3: Table look-up**	**Method 3 Graph, formula fit**
Apogee < 2 000 km	No	No	No margin req'd	5 % margin	10 % margin	25 % margin
Apogee < 2 000 km	No	Yes	No margin; use SRP	5 % margin; use SRP	10 % margin IFF $C_r \approx 1{,}7$	N/A
Apogee < 2 000 km	Yes	No	No margin req'd	5 % margin	N/A	N/A
Apogee < 2 000 km	Yes	Yes	No margin req'd; use SRP	5 % margin; use SRP	N/A	N/A
Apogee > 2 000 km	Either	Either	No margin req'd; use 3Bdy+SRP	5 % margin; use 3Bdy+ SRP	N/A	N/A

N/A = not applicable

3Bdy = third-body perturbations

SRP = solar radiation pressure

Method 1, certainly the highest fidelity model, utilizes a numerical integrator with a detailed gravity model, third-body effects, solar radiation pressure, and a detailed spacecraft ballistic coefficient model. Method 2 utilizes a definition of mean orbital elements,[4] [5] semi-analytic orbit theory and average spacecraft ballistic coefficient to permit the very rapid integration of the equations of motion while still retaining reasonable accuracy. Method 3 is simply a table lookup, graphical analysis or evaluation of formulae that have been fit to pre-computed orbit lifetime estimation data obtained via the extensive and repetitive application of Methods 1 and/or 2. It is worth noting that all methods (1 through 3) shall include at gravity zonals J_2 and J_3 at a minimum.

5.2 Method 1: High-precision numerical integration

Method 1 is the direct numerical integration of all accelerations in Cartesian space, with the ability to incorporate a detailed gravity model (e.g. using a larger spherical harmonics model to address resonance effects), third-body effects, solar radiation pressure, vehicle attitude rules or aero-torque-driven attitude torques, and a detailed spacecraft ballistic coefficient model based on the variation of the angle-of-attack, with respect to the relative wind. Atmospheric rotation at the Earth's rotational rate is also easily incorporated in this approach. The only negative aspects to such simulations are (a) they run much slower than Method 2, (b) many of the detailed data inputs required to make this method realize its full accuracy potential are simply unavailable, and (c) any gains in orbit lifetime prediction accuracy are frequently overwhelmed by inherent inaccuracies of atmospheric modelling and associated inaccuracies of long term solar activity predictions/estimates. However, to analyse a few select cases where such detailed model inputs are known, this is undoubtedly the most accurate method. At a minimum, Method 1 orbit lifetime estimations shall account for J_2 and J_3 perturbations and drag using an accepted atmosphere model and an averaged ballistic coefficient. In the case of high apogee orbits (e.g. geosynchronous transfer orbits) or other resonant orbits, sun and moon third-body perturbations and solar radiation pressure effects shall also be modelled (see Reference [28] for additional discussion).

5.3 Method 2: Rapid semi-analytical orbit propagation

Method 2 analysis tools utilize semi-analytic propagation of mean orbit elements[4] [5] influenced by gravity zonals J_2 and J_3 and selected atmosphere models. The primary advantage of this approach over direct numerical integration of the equations of motion (Method 1) is that long-duration orbit lifetime cases can be quickly analysed (e.g. 1 s versus 1 700 s CPU time for a 30-year orbit lifetime case). While incorporation of an attitude-dependent ballistic coefficient is possible for this method, an average ballistic coefficient is typically used. At a minimum, Method 2 orbit lifetime estimations shall account for J_2 and J_3 perturbations and drag using an accepted atmosphere model and an average ballistic coefficient. In the case of high apogee orbits (e.g. GTO), sun and moon third-body perturbations shall also be modelled.

5.4 Method 3: Numerical table look-up, analysis and fit formula evaluations

In this final method, one uses tables, graphs and formulae representing data that was generated by exhaustively using Methods 1 and 2 (see 5.2 and 5.3). The graphs and formulae provided in this International Standard can help the analyst crudely estimate orbit lifetime for their particular case of interest; the electronic access to tabular look-up provided via this International Standard (at www.CelesTrak.com) permits the analyst to estimate orbit lifetime for their particular case of interest via interpolation of Method 1 or Method 2 gridded data; all such Method 3 data in this International Standard were generated using Method 2 approaches. At a minimum, Method 3 orbit lifetime products shall be derived from Method 1 or Method 2 analysis products meeting the requirements stated above. When using this method, the analyst shall impose at least a 10 % margin of error to account for table look-up interpolation errors. When using graphs and formulae, the analyst shall impose a 25 % margin of error.

5.5 Orbit lifetime sensitivity to sun-synchronous

For sun-synchronous orbits, orbit lifetime has some sensitivity to the initial value of RAAN due to the density variations with the local sun angle. Results from numerous orbit lifetime estimations show that orbits with 6:00 am local time have longer lifetime than orbits with 12:00 noon local time by about 5,5 %.[3] This maximum difference (500 d) translates into a 5 % error which can be corrected by knowing the local time of the orbit. As a result, Methods 1 or 2 analyses of the actual sun-synchronous orbit condition shall be used when estimating the lifetime of sun-synchronous orbits (see References [28] and [38], where more details are given).

5.6 Orbit lifetime statistical approach for high-eccentricity orbits (e.g. GTO)

For high-eccentricity orbits (particularly geosynchronous transfer orbits or GTO), it can be difficult to iterate to lifetime threshold constraints due to the coupling in eccentricity between the third-body perturbations and the drag decay. Due to this convergence difficulty, only Method 1 or 2 analyses shall be used when determining initial conditions which achieve a specified lifetime threshold for such orbits.

Sample analyses of GTO launcher stages (see References [29] and [30]) highlight this orbit lifetime sensitivity to initial conditions (orbit, spacecraft characteristic and force model), leading to a wide spectrum of orbital lifetimes.

Some theoretical considerations about the dynamical properties of GTO orbits are provided in References [29] and [36].

The following test case illustrates the complex dynamical properties of GTO. Initial parameters are provided in Table 2.

Table 2 — GTO initial conditions for the Monte Carlo simulation

Perigee altitude	200 km
Apogee altitude	GEO altitude
Inclination	2°

Table 2 *(continued)*

Area to mass ratio	5e-3 m^2/kg
Solar activity	Constant (F10.7 = 140 sfu Ap = 15)
Drag coefficient	Constant = 2,2
Reflectivity coefficient	Constant = 2

Figure 4 shows lifetime results (years) when varying the initial date and the initial local time of perigee. This latest parameter is defined as the angle in the equator between the sun direction and the orbit perigee, measured in hours. The date was chosen from day 1 to 365 in year 1998 and the local time of perigee was chosen by varying the right ascension of ascending node from 0π to 2π. A total of 2 500 different initial conditions were generated.

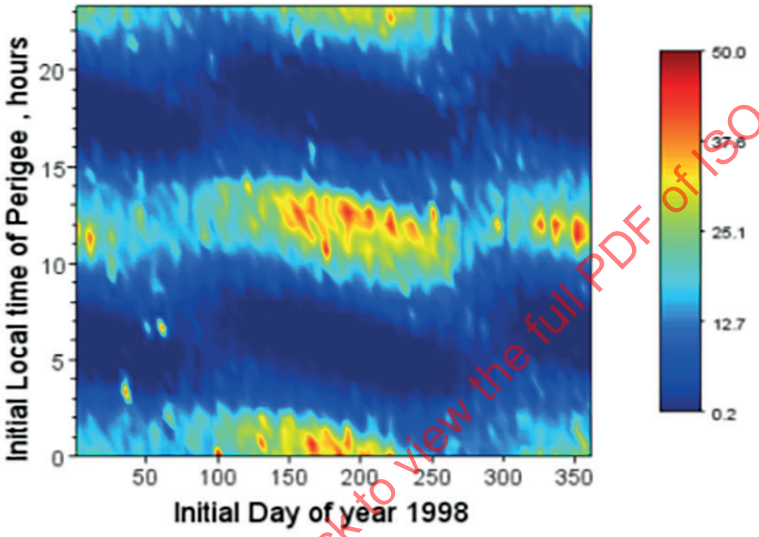

Figure 4 — Lifetime variations with respect to initial date and local time of perigee (year)

The shapes of the lifetime contours confirm that initial day of year and local time of perigee are initial conditions that make sense to describe GTO evolution since strong patterns are visible. The amplitudes of lifetimes variations are worth noting: from several months to more than 50 years. Previous results (see References [30] and [37]) are illustrated here: the longest lifetimes are obtained for initial sun-pointing (12 h local time) or anti sun-pointing (24 h local time) perigee with an initial date around the solstices. Note that the dark red pixels drawn in dark blue areas, as seen for initial day 60 and local time 7 h, are an indication of the presence of strong resonance phenomena. We know that the year also has an influence, to a lesser extent, through the moon perturbation.

Figure 5 shows semi-major axis evolution for several propagations of a typical low-inclined GTO. The different curves correspond to changes of 0,1 % or 1 % in the area to mass ratio of the object (A/m), which is far below the level of incertitude on this parameter. These dispersions lead to variations of decades in the re-entry duration. Such a strong non-linear behaviour is explained by the aforementioned resonances. One can see that semi-major axis evolutions are quite similar between all propagation cases until the entrance in the coupling between J2 and sun perturbations, for a semi-major axis equal to about 15 500 km. The duration of the resonance (period when the semi-major axis remains constant) and, thus, the rest of the propagation are completely different. A similar figure can be plotted by keeping the area to mass ratio constant and slightly changing the solar activity.

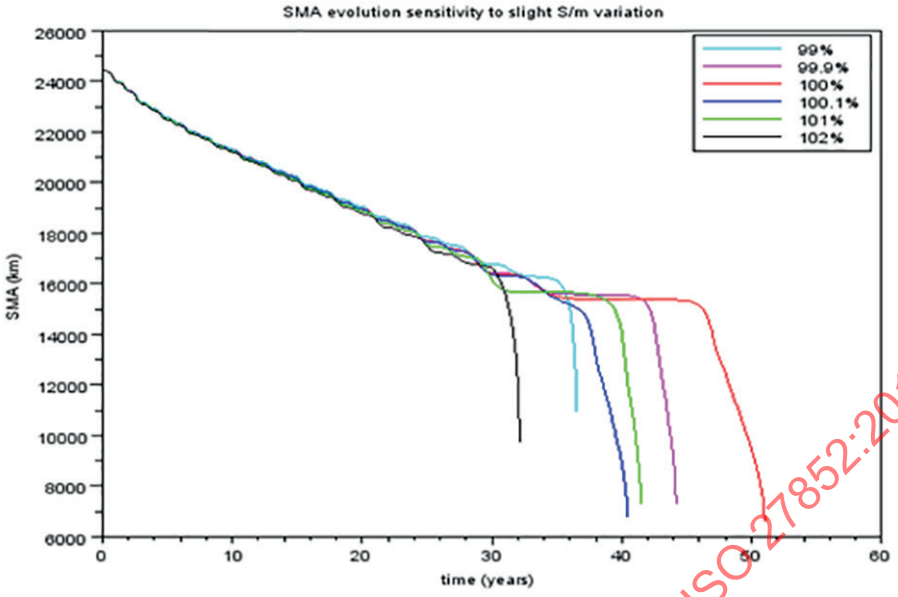

Figure 5 — SMA evolution sensitivity to slight A/m variations (from 0,1 to 2 %)

These examples show that resonance phenomena have substantial impacts on orbital elements evolution that can neither be predicted nor managed. Cumulated uncertainties on drag force between the extrapolation start (mission disposal manoeuvre, for example) and the instant when the resonance occurs make the entry condition in this resonance prone to strong variations. As a consequence, trying to estimate lifetime of GTOs using only one extrapolation may lead to erroneous conclusion since tiny changes in the initial conditions, spacecraft characteristics or force models end in very different lifetime results. Exceptions to that would be objects on a GTO whose semi major axis has already decreased enough to avoid resonances or to be very close to them. However, since resonance conditions change with regards to the possible resonant angles, one can see that performing several propagation cases is advised to get robust results. As a conclusion, only statistical results are adequate to estimate the strong variations of GTO lifetimes.

As a consequence, one should not say "this object's lifetime is Y years" in GTO but rather "the lifetime of this object is shorter than Y years with a probability p", coming from a cumulative distribution function (see example below).

The key parameter uncertainties to be taken into account in the lifetime estimation are

— initial conditions (date, orbit parameters),

— ballistic coefficient and drag coefficient, and

— solar activity.

The following test case (see Reference [32]) provides results of Monte Carlo simulations. Initial parameters are described in Table 3. A total of 2 500 different initial conditions were generated.

Table 3 — Hypothesis for the Monte Carlo simulation

Parameter	Nominal value	Dispersions
Perigee altitude	180 km	Small dispersions : 1sigma standard deviation about 1 km, correlated to other orbit parameters.
Apogee altitude	GEO altitude	Small dispersions: 1sigma standard deviation about 50 km, correlated to other orbit parameters.
Inclination	6°	Small dispersions: 1sigma standard deviation about 0,01°, correlated to other orbit parameters.
Area to mass ratio	5e-3 m^2/kg	Uniform distribution +/–20 % wrt nom. value
Drag coefficient	Function of geodetic altitude	None
Reflectivity coefficient	Constant = 1,5	None
Solar activity	Randomly chosen using data from the past	
Date	Uniform distribution between day 1 to day 365, for years between 2015 and 2033 (the dispersion of the year enables to cover the moon perturbation).	
Local time of perigee	Gaussian distribution, mean value 22 h standard deviation 50 min	

Figure 6 and Figure 7 provide a statistical histogram and cumulative distribution function of orbit lifetime for this test case.

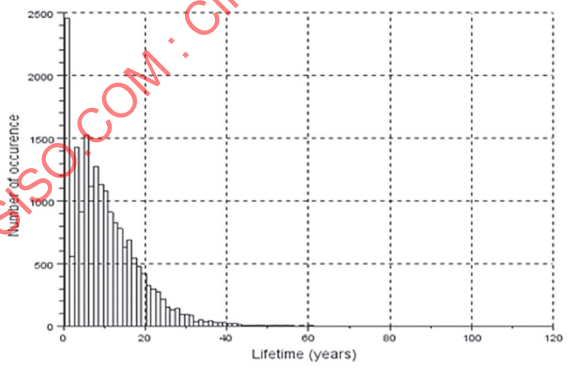

Figure 6 — Histogram of orbital lifetimes

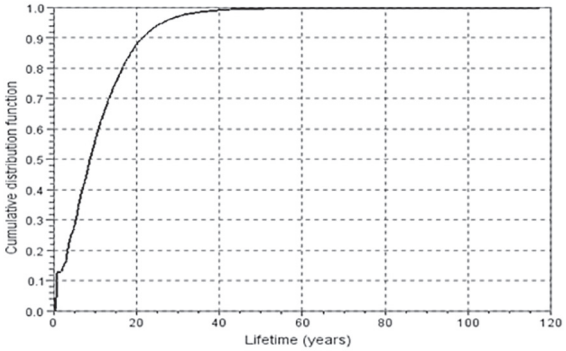

Figure 7 — Cumulative distribution function of orbital lifetimes

The question of statistical convergence may be addressed by computing a confidence interval for the Monte Carlo results, associated to a confidence level. The so-called "interval of Wilson with correction for continuity" (see Reference [31]) has been well-adapted for this purpose.

In this approach, the upper $p1$ and lower $p2$ limits of this interval are given by Formula (1):

$$p1 = \frac{2nf + u_{a/2}{}^2 - 1 - u_{a/2}\sqrt{u_{a/2}{}^2 - 2 - 1n + 4f[n(1-f)+1]}}{2(n + u_{a/2}{}^2)}$$
$$p2 = \frac{2nf + u_{a/2}{}^2 - 1 - u_{a/2}\sqrt{u_{a/2}{}^2 - 2 - 1n + 4f[n(1-f)-1]}}{2(n + u_{a/2}{}^2)} \quad (1)$$

where

n is number of single runs (orbit propagations);

f is observed probability = number of lifetimes lower than a certain value divided by n;

$u_{\alpha/2} = \Phi^{-1}(1- \alpha/2)$ (= 1,96, for example, for a confidence interval of 95 %). Φ is the cumulative normal distribution function.

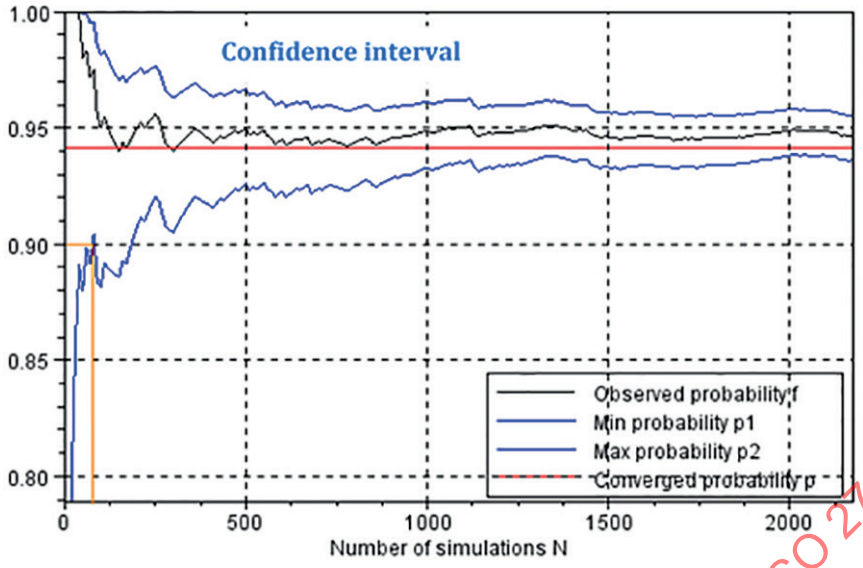

Figure 8 — Example of evolution of the observed probability (lifetimes lower than 25 years) and 95 % confidence interval

As shown in Figure 8 and Figure 9, after "N" Monte Carlo runs, one can compare the limit (upper or lower) of the confidence interval with the targeted probability for the lifetime to be lower than a certain value.

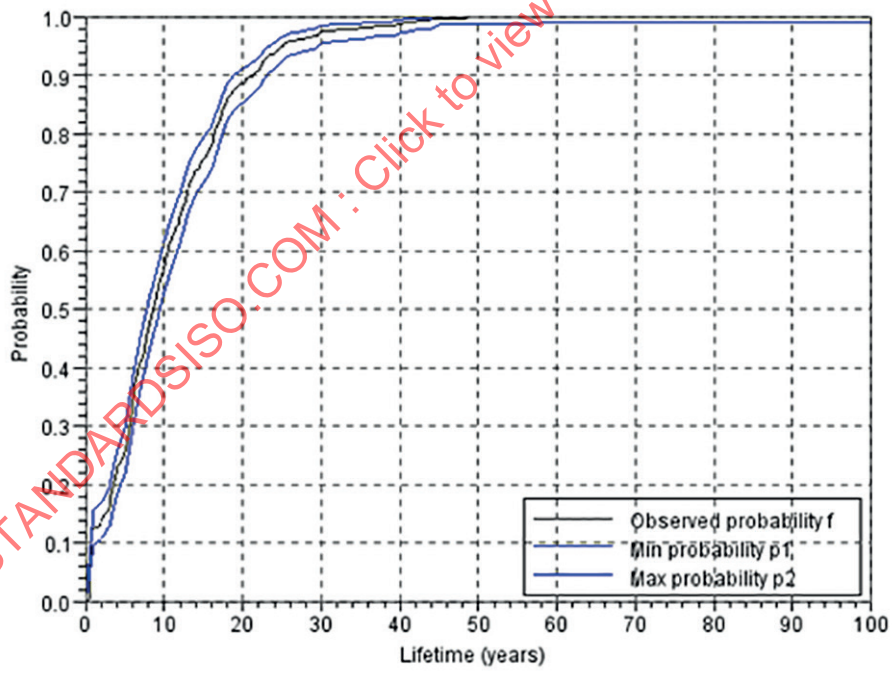

Figure 9 — Example of cumulative distribution function of orbital lifetimes with a 95 % confidence interval (500 runs)

6 Drag modelling

6.1 General

The three biggest factors in orbit lifetime estimation are (a) the selection of an appropriate atmosphere model to incorporate into the orbit acceleration formulation, (b) the selection of appropriate atmosphere model inputs, and (c) determination of a space object's ballistic coefficient. We will now spend some time discussing each of these three aspects.

6.2 Atmospheric density modelling

There are a wide variety of atmosphere models available to the orbit analyst. The background, technical basis, utility and functionality of these atmosphere models are described in detail in References [6] to [15]. This International Standard will not presume to dictate which atmosphere model the analyst shall use. However, it is worth noting that in general, the heritage, expertise and especially the observational data that went into creating each atmosphere model play a key role in that model's ability to predict atmospheric density, which is in turn, a key factor in estimating orbit lifetime. Many of the early atmosphere models were low fidelity and were created on the basis of only one, or perhaps even just a part of one, solar cycle's worth of data.

The advantage of some of these early models is that they typically run much faster than the latest high-fidelity models (see Table 4) without a significant loss of accuracy. However, the use of atmosphere models that were designed to fit a select altitude range (e.g. the "exponential" atmosphere model depicted below) or models that do not accommodate solar activity variations should be avoided as they miss too much of the atmospheric density variations to be sufficiently accurate.

There are some early models (e.g. Jacchia 1971 shown below) which accommodate solar activity variations and also run very fast; these models can work well for long-duration orbit lifetime studies where numerous cases are to be examined. Conversely, use of the more recent atmosphere models are encouraged because they have substantially more atmospheric drag data incorporated as the foundation of their underlying assumptions. A crude comparison of a sampling of atmosphere models for a single test case is shown in Figure 10 and Figure 11, illustrating the range of temperatures and densities exhibited by the various models. Although this International Standard does not presume to direct which atmosphere model the analyst should use, the reader is encouraged to seek atmosphere model guidance from ISO 14222 to select proper atmosphere and associated indices. However, it is also noted that the lengthy prediction timespan associated with this International Standard makes a number of atmosphere models suitable for estimation of orbital lifetimes spanning 25 years, to include, but not limited to, the NRLMSISE-00,[10] JB2006,[11] JB2008,[12] GRAM-07,[13] DTM-2000[14] and GOST[15] models.

Table 4 — Comparison of normalized density evaluation runtimes

Atmosphere model	0 < Alt < 5 000 km	0 < Alt < 1 000 km
Exponential	1,00	1,00
Atm1962	1,43	1,51
Atm1976	1,54	1,54
Jacchia 1971	13,68	17,31
MSIS 2000	141,08	222,81
JB2006	683,85	584,47

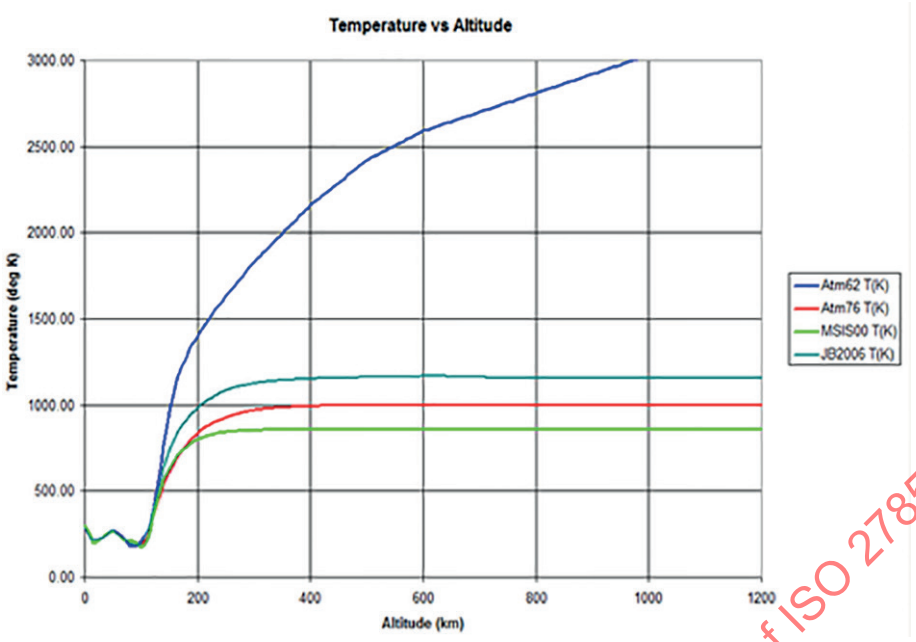

Figure 10 — Temperature comparison by atmosphere model

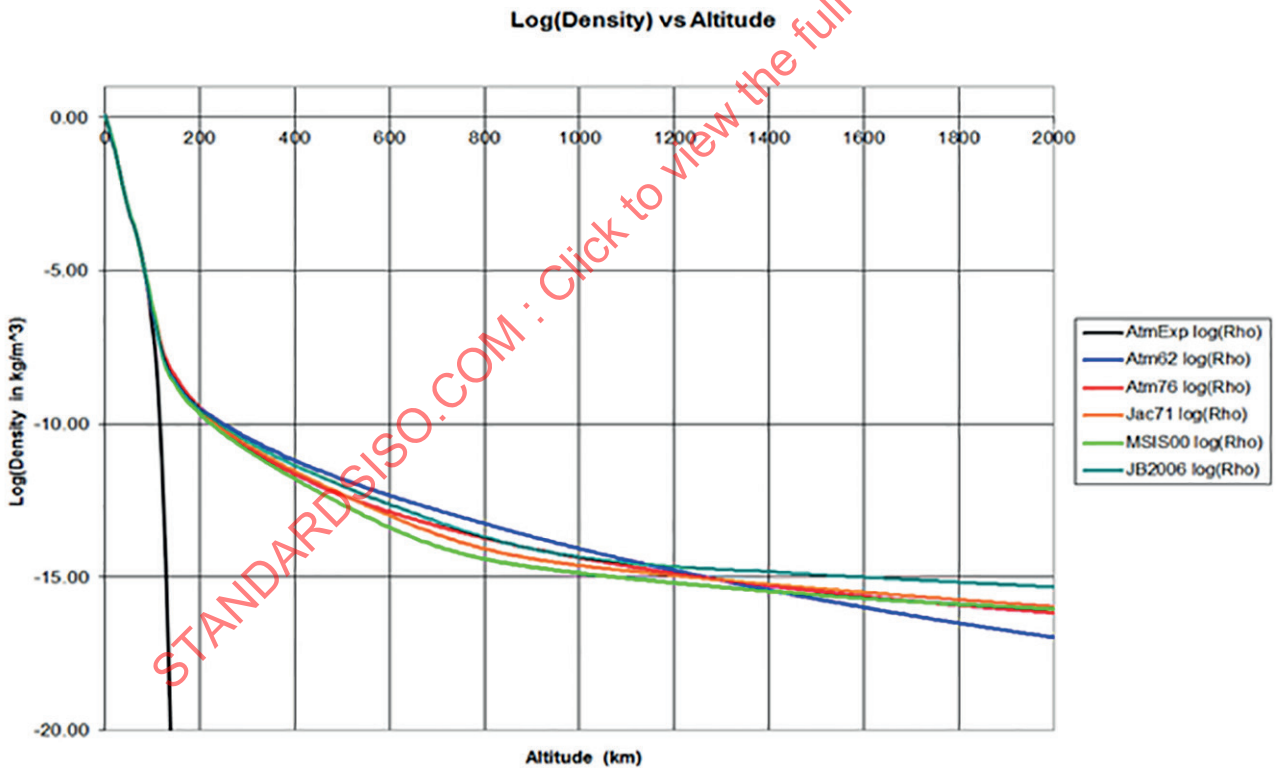

Figure 11 — Comparison of a small sampling of atmosphere models

6.3 Long-duration solar flux and geomagnetic indices prediction

Utilization of the higher-fidelity atmosphere models mentioned in 6.2 requires the orbit analyst to specify the solar and geomagnetic indices required by such models. Care must be taken to obtain the proper indices required by each model; subtle difference may exist in the interpretation of similarly named indices when used by different atmosphere models (e.g. centrally-averaged vs. backward-averaged $F_{10,7}$ Bar).

Key issues associated with any prediction of solar and geomagnetic index modelling approach are as follows.

a) $F_{10,7}$ Bar predictions should reflect the estimated mean solar cycle as accurately as possible. One such prediction is shown in Figure 12.

b) Large daily $F_{10,7}$ and A_p index variations about the mean value induce non-linear variations in atmospheric density and the selected prediction approach should account for this fact, i.e. one should account for the highly non-linear aspects of solar storms versus quiet periods.

c) The frequency of occurrence across the day-to-day index values is highest near the lowest prediction boundary (see Figure 13).

d) $F_{10,7}$ cycle timing/phase is always imprecise and should be accounted for; the resultant time bias that such a prediction error would introduce can yield large $F_{10,7}$ prediction errors of 100 % or more.

e) The long-time duration orbit lifetime constraint specified in ISO 24113 (i.e. 25 years) would require that the solar/geomagnetic modelling approach provide at least that many years (i.e. 25) of predictive capability.

f) Predicted $F_{10,7}$ values should be adjusted to correct for earth-sun distance variations.

g) Some atmosphere models (e.g. JB2006 and JB2008), due to the newly invented indices adopted thereby, preclude the use of historical indices for long-term orbit lifetime studies while currently also precluding use of any predictive forecasting model(s) for those indices until such time as those become publicly available.

Accounting for these constraints, the user shall adopt one of the following three acceptable approaches.

— Approach #1: Utilize Monte Carlo sampling of historical data[16] [17] mapped to a common solar cycle period.

— Approach #2: Utilize a predicted $F_{10,7}$ Bar solar activity profile generated by a model such as is detailed[19] in Figure 12, coupled with a stochastic or similar generation of corresponding $F_{10,7}$ and A_p values, e.g. Reference [19].

— Approach #3: Utilize a "Mean Equivalent Static" set of solar and geomagnetic activity. Note that while such an approach produces equivalent solar and geomagnetic indices that are suitable for efficient and equivalent orbit lifetime estimation, such static values are only valid for the cycles fit, the selected orbit prediction span (i.e. 25 years) with an associated probability level and the adopted atmosphere model. New sets of Mean Equivalent Static indices would likely need to be generated for any changes in the above functional dependencies.

Since Approach #2 is a well-known and common approach, the focus of the remainder of this subclause will be devoted to (Approach #1) the Monte Carlo "Random Draw" approach[3] and the "Mean Equivalent Static" approach (Approach #3).

6.4 Approach 1: Monte Carlo random draw of solar flux and geomagnetic indices

Note (see Figure 2) that we already have more than five solar cycles of observed solar and geomagnetic data to choose from. Processing of this data maps each coupled and correlated triad of datum ($F_{10,7}$, $F_{10,7}$ Bar, and A_p) into a single solar cycle range of 10,825 46 years (3 954 d), with the "averaged" solar minimum referenced to 25 February 2007.

By mapping this historical data into a single solar cycle (see Figure 14 through Figure 16), the user can then sample coupled triads of ($F_{10,7}$, $F_{10,7}$ Bar, and A_p) data corresponding to the orbit lifetime simulation day within the mapped single solar cycle. This solar/geomagnetic data can then be updated at a user-selectable frequency (e.g. once per orbit or day), thereby simulating the drag effect resulting from solar and geomagnetic variations consistent with historical trends for these data. Since we have accumulated daily data since the February 14, 1947, on any given day within the 3 954-day solar cycle, we have at

least five data triads to choose from. It is important that the random draw retain the integrity of each data triad since $F_{10,7}$, $F_{10,7}$ Bar and A_p are interrelated.

In the Monte Carlo approach for modelling solar and geomagnetic data, coupled triads of ($F_{10,7}$, $F_{10,7}$ Bar, and A_p) data are selected for each day (or alternately for each orbit rev) of the orbit lifetime simulation, thereby simulating the drag effect resulting from solar and geomagnetic variations consistent with historical trends for these data. The atmospheric density estimated from atmospheric models utilizing a given ($F_{10,7}$, $F_{10,7}$ Bar, and A_p) triad can then be directly utilized by either Method 1 (numerical integration) or Method 2 (semi-analytic) approaches. Due to the introduced step-function change in atmospheric density, it may be beneficial to restart Method 1 integration at each parameter set change; for semi-analytic (e.g. with orbital revolution time steps via Gaussian quadrature), a new parameter set can be drawn at an orbit revolution time step; thus, no numerical difficulties will be introduced.

The starting epoch of the simulation can be selected to match the anticipated actual end-of-mission epoch. Alternately, starting epochs can be sampled throughout the entire aggregate solar cycle and to ensure that the median (50th-percentile) value meets the specified orbit lifetime criteria of ISO 24113. The C++ code used to implement this atmospheric variation strategy is publicly available at www.CelesTrak.com so that users of this orbit lifetime standard can adopt this standardized ($F_{10,7}$, $F_{10,7}$ Bar and A_p) implementation Approach #1 if desired.

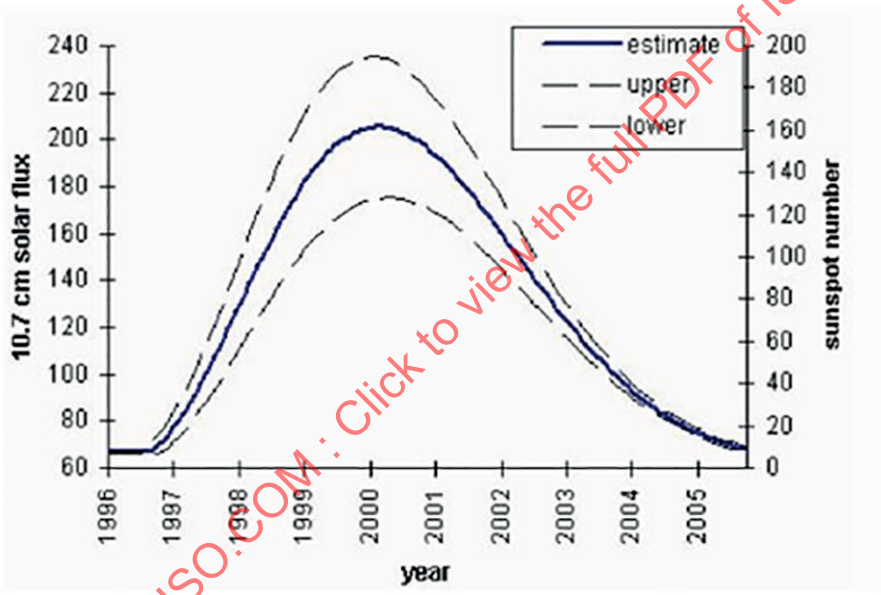

Figure 12 — Solar flux estimated upper, lower and representative trends

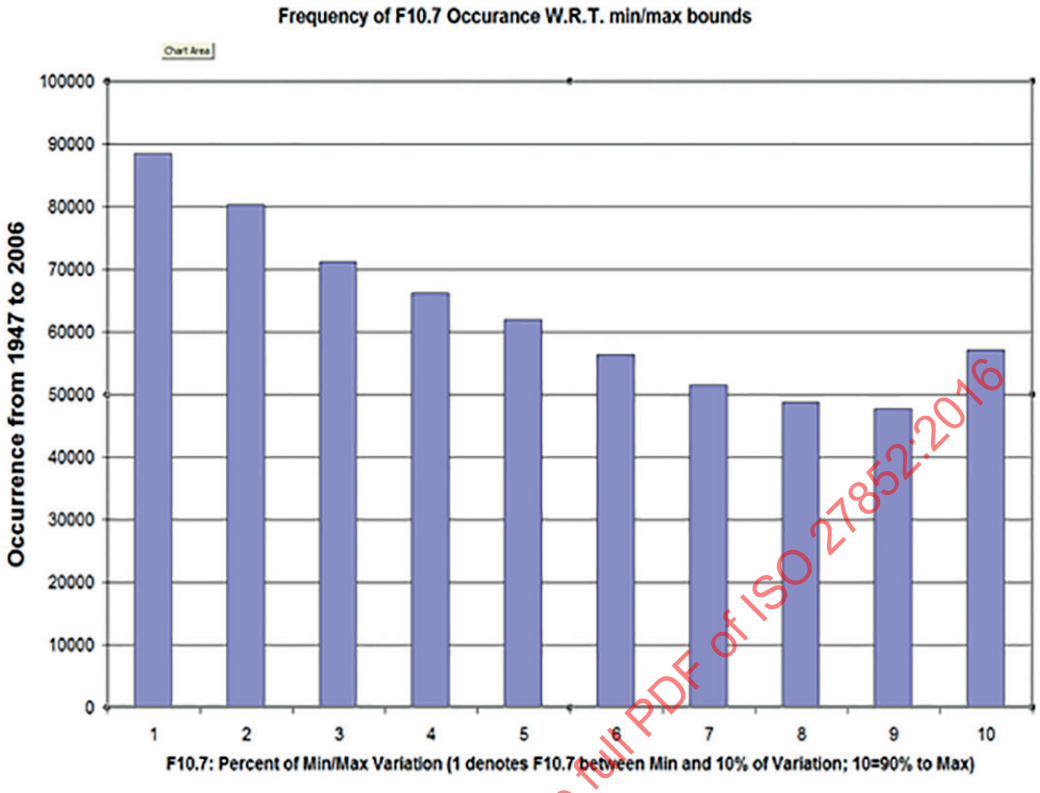

Figure 13 — Solar flux distribution in percentage of localized min/max variation

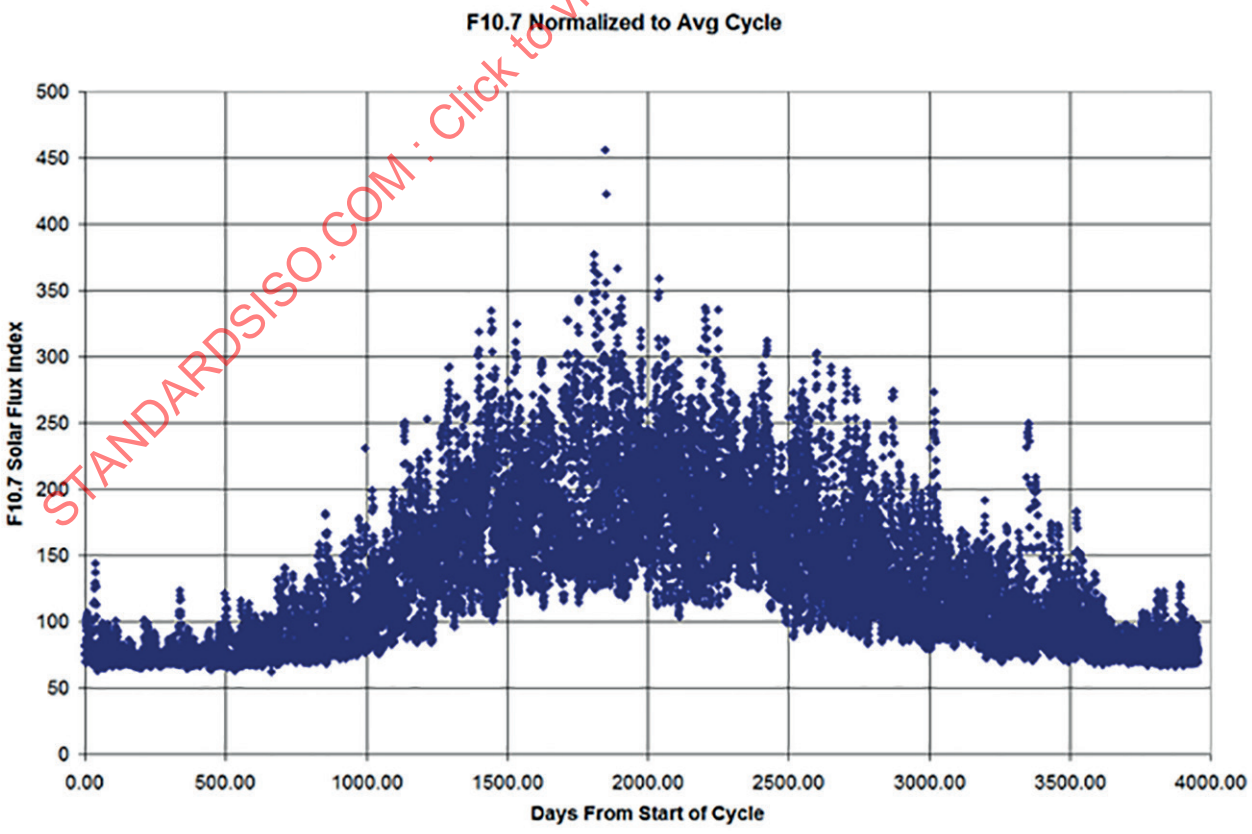

Figure 14 — F10.7 normalized to average solar cycle

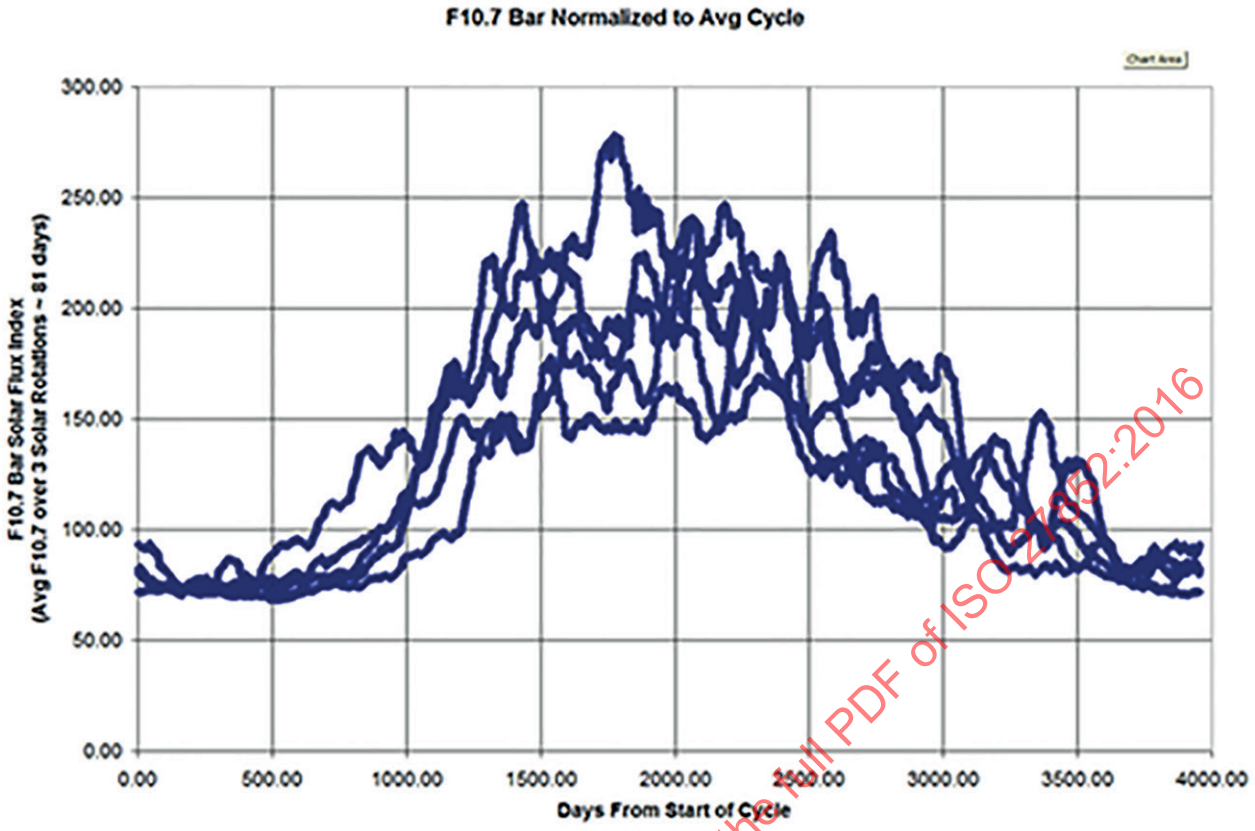

Figure 15 — F10.7 bar normalized to average cycle

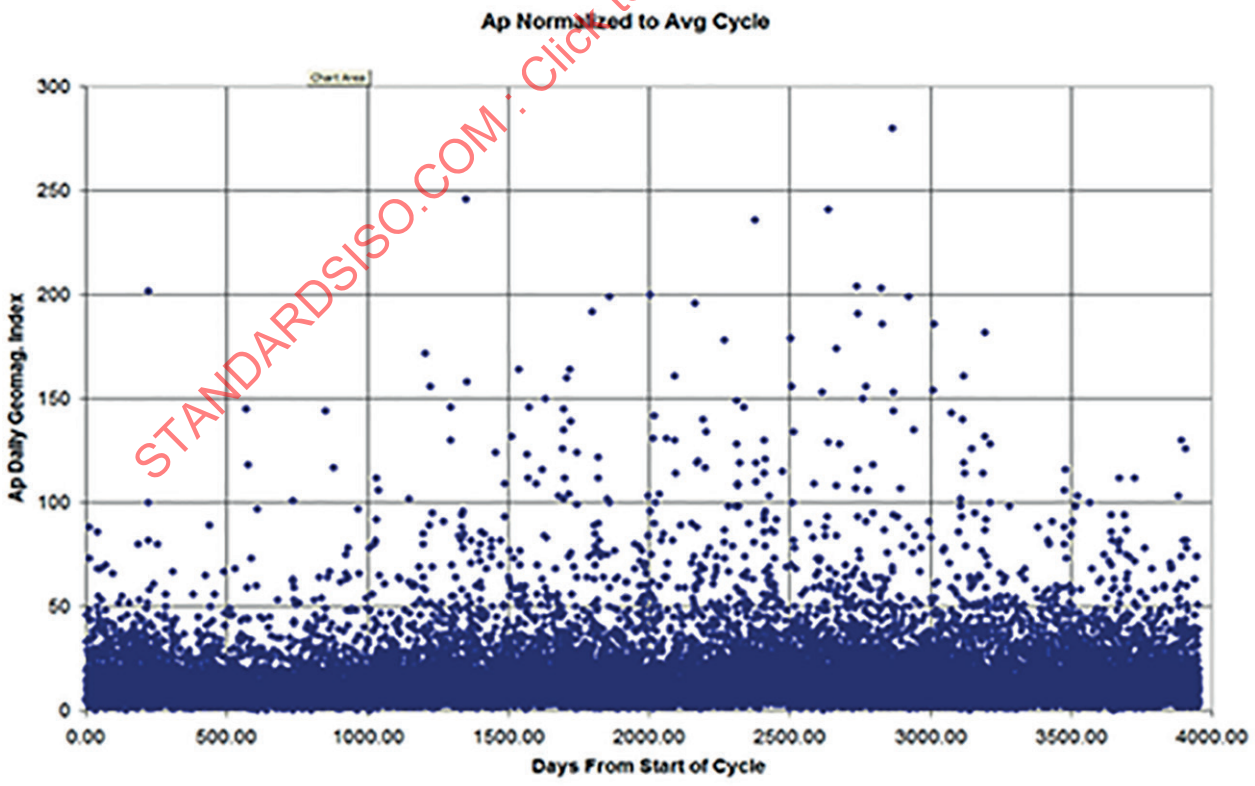

Figure 16 — A_p normalized to average cycle

It can be seen from Figure 16 that A_p is (a) unpredictable, (b) loosely correlated with the solar cycle, and (c) volatile. Figure 17 demonstrates that density varies greatly (i.e. several orders of magnitude) depending upon A_p; thus, a geomagnetic storm can induce large decreases in orbital energy (orbit decay) that the use of some average A_p value would miss. Correspondingly, the analyst should incorporate A_p variations into the geomagnetic index predictions.

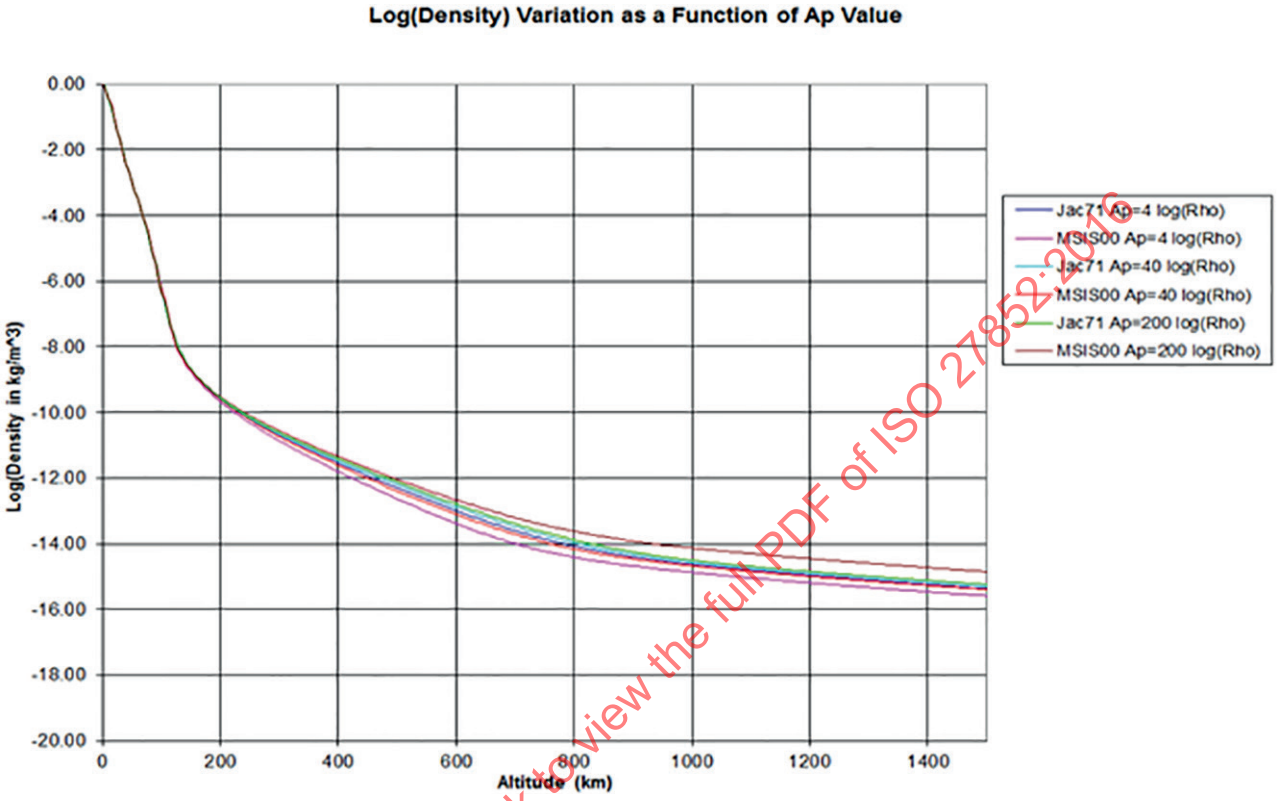

Figure 17 — Log (density) variation as a function of A_p value

6.5 Method 3: Equivalent constant solar flux and geomagnetic indices

A third method for simulation of solar flux and geomagnetic indices is the use of "Equivalent Constant Solar Flux and Geomagnetic Indices." In this method, the user generates (or obtains from a qualified third party) and incorporates pre-computed constant equivalent values of solar flux and geomagnetic activity into the orbit lifetime estimation process which will yield the same orbital lifetime as would the use of actual measured (dynamic) indices. Since the starting epoch with respect to solar cycles may be not well known and is a sensitive parameter of orbit lifetime estimation (about ±4 years for a typical LEO orbit), the starting epoch can be included in the Monte Carlo as a random parameter (the initial day is a random realization within the first solar cycle). This pre-computation of equivalent constant indices avoids the use of random draws each orbit and repeated Monte Carlos for the actual orbit of interest.

If Method 3 is employed, the equivalent constant indices shall be carefully tuned by the analyst to match historical solar and geomagnetic influences on orbit decay over a long-duration (i.e. 25-year) timespan corresponding to the atmosphere model and orbit inclination of interest. This ensures that a space object having a specific ballistic coefficient and starting orbit that has a 25-year lifetime computed by using the constant equivalent solar activity yields an orbit lifetime estimate of less than 25 years with a z % probability level (see Figure 22).

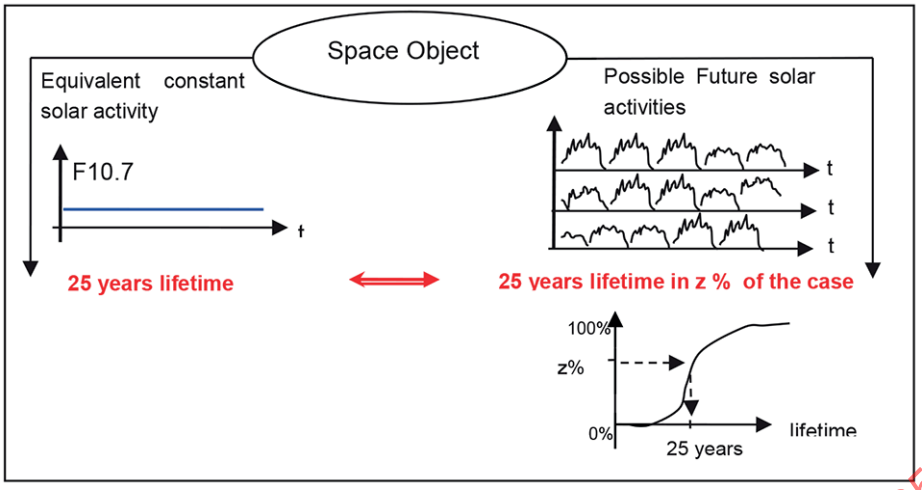

Figure 18 — Statistical equivalency between constant and variable solar activity

Equivalent constant solar flux and geomagnetic activity indices are obtained via the following algorithm.

a) Select the initial orbit and a ballistic coefficient.

b) Select a representative geomagnetic A_p index (e.g. 15).

NOTE As there are two uncertain parameters (solar flux and geomagnetic index) with no evident correlation between them, this method is faced with two degrees of freedom versus only one output (estimated orbit lifetime). The method circumvents this by adopting a representative geomagnetic A_p index value which is averaged over the timespan of interest (e.g. 25 years).

c) Using the random draw Monte Carlo approach previously outlined (see Method #1), generate n possible future solar activities (including random draws of starting date which encompass all possible launch dates, including launch slips).

d) Estimate orbit lifetime using the solar activity profiles, where n is appropriately sized using Dagum (Chernoff – Hoeffding) bounding methods.

e) As shown in Figure 23 and adopting z % to be 50 % (the median value), determine OLT_50 % (the median orbit lifetime of the trials).

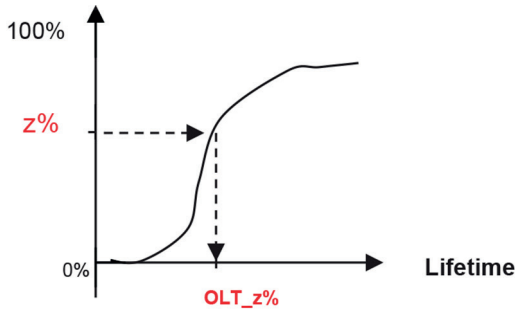

Figure 19 — Lifetime cumulative distribution function

f) Iterate on either initial orbit semi-major axis or perigee altitude until an OLT_50 % of 25 years is found. At every step, estimate n orbit lifetimes using new (randomly-drawn) solar activity profiles. The orbit that has an OLT_50 % of 25 years is called the end-of-life limiting orbit.

g) Using the solved-for end-of-life limiting orbit, determine by iteration the constant equivalent solar flux index (F10,7_50 % as shown in Figure A.1) which also yields an orbit lifetime of 25 years.

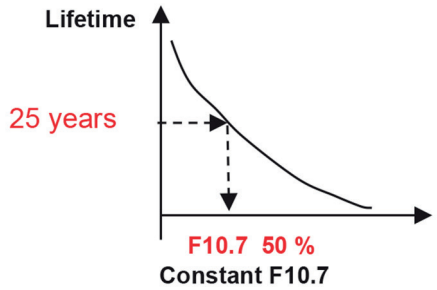

Figure 20 — F10.7_z % value computation

h) Determine the viability region of the solved-for F10,7_z % value as a function of:

1) initial orbit inclination,
2) orbit eccentricity,
3) ballistic coefficient of the space object,
4) local time of the ascending node, and
5) atmosphere model.

i) It is the task of the analyst to ensure that the equivalent constant solar activity values or expressions derived through these steps are applicable to the end-of-mission orbits to be analysed.

j) Parametric runs can be used to yield functional relationships for constant equivalent solar flux as a function of ballistic coefficient, orbit altitude(s), inclination, etc. One such expression for constant equivalent ("mean equivalent static") solar activity has defined as follows:[34]

$$AP = 15$$
$$F_{10,7} = 201 + 3,25\ \ln\left(\frac{AC_d}{m}\right) - 7\ln(Z_a) \quad (2)$$

where

AP is the geomagnetic index value to be used by the atmospheric model;

$F_{10.7}$ is the solar flux value (in SFUs) to be used by the atmospheric model;

AC_d/m is ballistic coefficient (m^2/kg);

Z_a is apogee radius (mean parameter) minus earth radius (6 378 km), Za < 2 200 km.

Note that for extrapolation using a variable drag coefficient vs altitude, a constant value of C_d shall be used to compute the constant equivalent solar activity. A C_d value of 2,2 has been chosen but the analyst is encouraged to select a more appropriate value if warranted.

Figure A.2 shows a plot of $F_{10.7}$ values using the above parametric function for several ballistic coefficients and apogee altitudes.

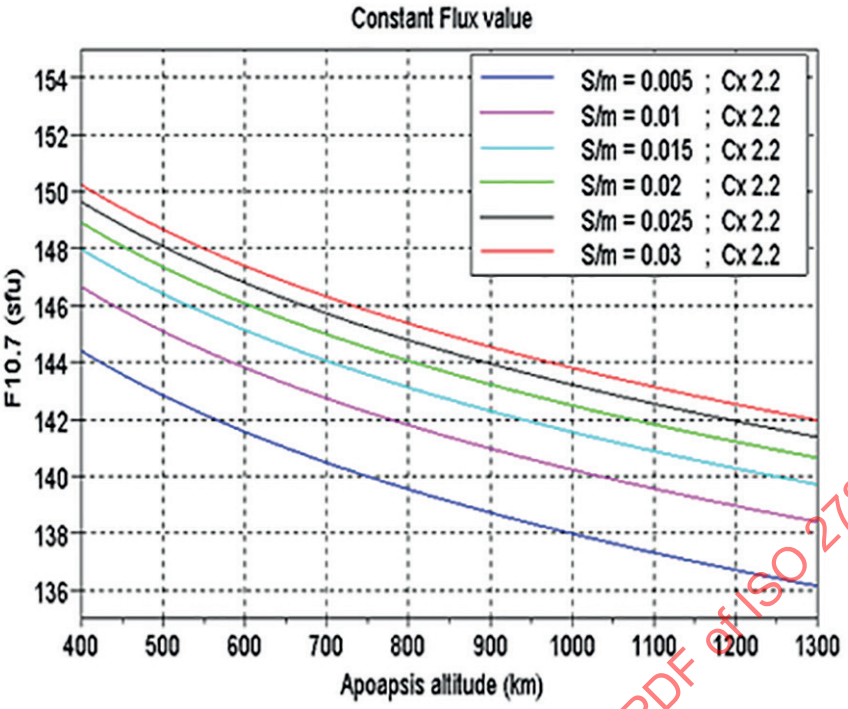

Figure 21 — Constant equivalent flux values

If done correctly, the Monte Carlo Approach #1 (random draws of initial date and solar activity) and Approach #3 (equivalent constant solar flux index) should yield the same orbit lifetime.

Figure 22 is a typical LEO cumulative distribution function of lifetimes considering random initial date and solar activity (Monte Carlo). The perigee has been tuned to obtain p = 0,5 for 25 years. The same 25 years lifetime is obtained with one run considering the constant equivalent solar activity.

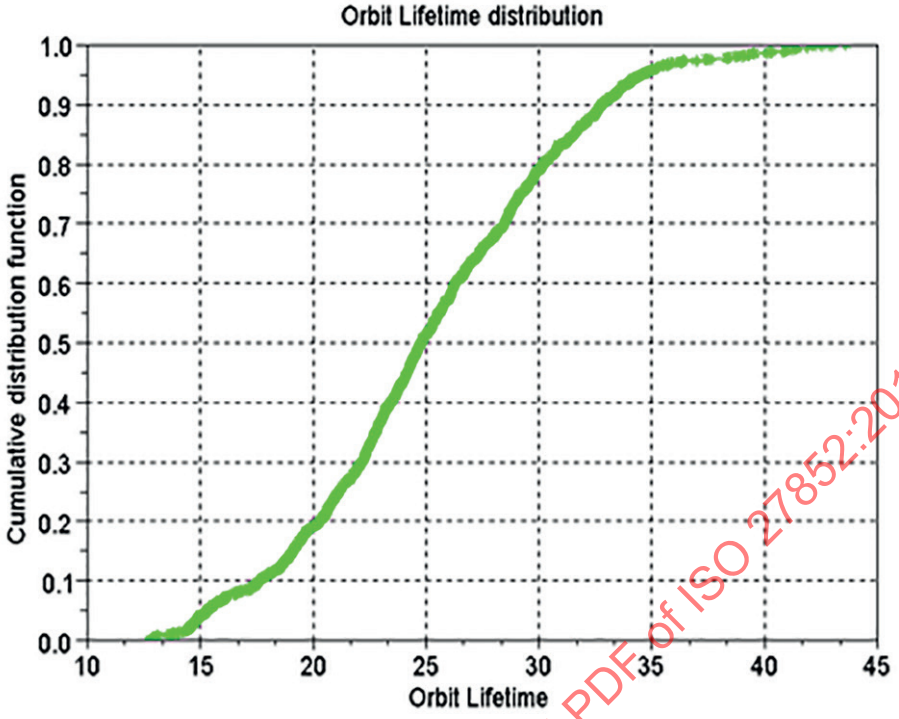

Figure 22 — Typical LEO cumulative distribution function considering random initial date and solar activity

6.6 Atmospheric density implications of thermospheric global cooling

Recent indications of global cooling in the thermosphere may have gradually increasing role in orbit lifetime estimation. The thermosphere is defined to occur roughly between 80 km and 500 km altitude, which is a key part of the LEO regime for which the ISO standard is being developed. Both spacecraft measurements[14] and theoretical models[15] [16] indicate that the thermosphere is cooling off, causing density to lower. The mechanism causing this change appears to be that as CO_2 concentrations have increased (from 320 ppmv in 1965 to around 380 ppmv in 2005) at altitudes below 30 km and the upper atmosphere is correspondingly cooling down. It is estimated that because of this effect, atmospheric density will decrease by between 1,7 %[20] and 2 %[21] [22] per decade. This decrease yields a corresponding increase in orbit lifetime of between 4 % and 7 %.[2]

7 Estimating ballistic coefficient ($C_D A/m$)

7.1 General

The first step in planning a LEO-crossing space object disposal is to estimate the ballistic coefficient ($C_D A/m$), β where:

β = (Coefficient of Drag C_D) × (Object Cross-Sectional Area)/Object Mass

Accurate estimation of the space object's ballistic coefficient is another key element in the orbit lifetime analysis process. Frequently, the analyst will select an average ballistic coefficient for the duration of the prediction but this is not always the case. We will examine cross-sectional area and drag coefficient estimations separately. Spacecraft mass shall be varied according to best-available knowledge but may typically be assumed to be constant from end-of-life until orbit decay.

7.2 Estimating aerodynamic force and SRP coefficients

A reasonable value of the dimensionless drag coefficient, C_D, is 2,2 for a typical spacecraft. However, the drag coefficient, C_D, depends on the shape of the spacecraft and the way air molecules collide with it. For certain geometric configurations such as spheres, cylinders and cones, the value of axial drag coefficient, C_D, can be evaluated more precisely than previously noted provided something is known about the flow regime and reference area. The analyst shall consider C_D variations based on spacecraft shape and anticipated uncontrolled attitudinal stability. The drag coefficient can become considerably higher than 2,2 for elongated spacecraft shapes; for those shapes, a more accurate result can be obtained by using the "panel model" described below.

For long-duration orbit lifetime estimations, C_D variation as a function of attitude and orbit altitude may potentially be ignored since the orbit lifetime percent error may be quite small due to averaging effects over very long-duration (e.g. 25 years) orbit lifetime time spans.

7.2.1 Aerodynamic and solar radiation pressure coefficient estimation via a "panel model"

If the spacecraft shape is not overly complex, aerodynamic force and SRP coefficients may be estimated quite well using a spacecraft panel model (see References [39], [40] and [41]). A panel model consists in its simplest form of a set of $I = 1, \ldots, N$ panels, each panel described only by its area Ai and its outward normal unit vector $\hat{n}_i$ that defines its orientation in a spacecraft body-fixed frame.

These models do not provide information on the shape and relative position of each panel. Obscuration of one panel by another is not incorporated into this simple panel model. Finer detail of the spacecraft surface, such as protruding antennae, star camera baffles, etc., are either neglected or could be handled by slightly adjusting the parameters of the larger flat surfaces.

For such panel models, the radiation pressure force coefficient vector for the entire spacecraft can be computed by simply summing the panel contributions, as follows:

$$C_r = \sum_i C_{r,i} \tag{3}$$

For calculating the aerodynamic force coefficient using such a panel model, a double summation is necessary, both over the spacecraft panels i, and over the atmospheric constituents j. In addition, the contributions of drag and lift were computed separately and now need to be summed as well.

$$\bar{C}_a = \sum_i \sum_j \left(\frac{\rho_j}{\rho}\right)\left(C_{D,i,j}\hat{u}_D + C_{L,i,j}\hat{u}_{L,i}\right) \tag{4}$$

where $\left(\frac{\rho_j}{\rho}\right)$ represents the relative mass concentrations of the different particles species (j = O2,N2, O, He, H, . . .) having different molecular masses m_j. The drag direction $\hat{u}_D$ is determined from the relative velocity vector v_r as:

$$\hat{u}_D = \frac{v_r}{\|v_r\|} \tag{5}$$

The unit vector for the lift and side force direction, $\hat{u}_{L,i}$, is perpendicular to $\hat{u}_D$ and in the plane spanned by $\hat{n}_i$ (normal to panel "i") and $\hat{u}_D$.

$$\hat{u}_{L,i} = -\frac{\left(\hat{u}_D \times \hat{n}_i\right) \times \hat{u}_D}{\left\|\left(\hat{u}_D \times \hat{n}_i\right) \times \hat{u}_D\right\|} \tag{6}$$

Drag and lift coefficients may be determined from:

$C_D = \bar{C}_a \cdot \hat{u}_D$ and $C_L = \left|\bar{C}_a - C_D \hat{u}_D\right|$, with lift being in the unit direction of $\dfrac{\bar{C}_a - C_D \hat{u}_D}{\left|\bar{C}_a - C_D \hat{u}_D\right|}$ (note that lift could be zero, such that the programmer should guard against division by zero in this last formula).

To feed the above formulae, each panel's drag coefficient and combined lift and side force coefficient are determined from:

$$C_{D,i,j} = \left[\frac{P_{i,j}}{\sqrt{\pi}} + \gamma_i Q_j Z_{i,j} + \frac{\gamma_i}{2}\frac{v_{re}}{v_{inc}}\left(\gamma_i \sqrt{\pi} Z_{i,j} + P_{i,j}\right)\right]\frac{A_i}{A_{\text{ref}}} \tag{7}$$

$$C_{L,i,j} = \left[l_i G_j Z_{i,j} + \frac{l_i}{2}\frac{v_{re}}{v_{inc}}\left(\gamma_i \sqrt{\pi} Z_{i,j} + P_{i,j}\right)\right]\frac{A_i}{A_{\text{ref}}} \tag{8}$$

where

$$\gamma_i = \cos\left(\theta_i\right) = -\hat{u}_D \cdot \hat{n}_i$$

$$l_i = -\hat{u}_L \cdot \hat{n}_i$$

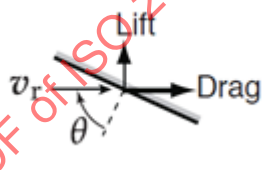

$$S_j = \frac{v_r}{\sqrt{2\left(\dfrac{R}{0{,}001\,\text{m}_j\left(u\right)}\right)\left(\text{Temperature}\right)}}$$

$$G_j = \frac{1}{2S_j^2}$$

$$P_{i,j} = \frac{1}{S_j} e^{-\gamma_i{}^2 S_j^2}$$

$$Q_j = 1 + G_j$$

$$Z_{i,j} = 1 + \text{erf}\left(\gamma_i S_j\right)$$

$$\frac{v_{re}}{v_{inc}} = \sqrt{\frac{1}{2}\left[1 + \propto\left(\frac{4RT_W}{0{,}001\,\text{m}_j\left(u\right)v_r{}^2} - 1\right)\right]}$$

A_{ref} is the reference area of the spacecraft and should be a positive constant during the whole computation of drag on a panel model. An averaged spacecraft cross-sectional area is commonly adopted for A_{ref}.

Also, $\propto$ = accommodation coeff., T_W = Wall Temp in deg *K*, *R* – Univ. Gas Constant.

Note that the unit vector in the drag direction depends only on the relative velocity and is independent of the panel orientation and therefore does not carry the index *i*. Depending on the orientation of the 2D panel within the 3D spacecraft model, the lift contribution of each panel, in the direction $\hat{u}_{L,i}$ shall result in a combined aerodynamic lift and side force.

As an example, we examine the aerodynamic force coefficient for a single plate having an area of 1,0 m^2. We then consider three panel orientations w.r.t. the drag vector (i.e. θ_i, the angle between the panel inward normal and the drag vector of 0°, 45° and 90°). For this example, we also adopt the following conditions and examine only the oxygen component:

$A_{\text{ref}} = 1\ \text{m}^2$, $T_{\text{w}} = 300\ K$, $R = 8{,}314\ 462\ 1\ \frac{J}{K\ mol}$, $\propto = 1$, $T = 1\ 000\ K$, $m_j = 16\ u$ (*atomic Oxygen*)

$v_r = 7\ 600$ m/s

For these conditions, we obtain the following:

Parameter	$\theta_i = 0°$	$\theta_i = 45°$	$\theta_i = 90°$
Y_i	1,0	0,707 106 78	0,0
l_i	0,0	0,707 106 78	1,0
S_j	7,454 894	7,454 894	7,454 894
G_j	0,008 996 8	0,008 996 8	0,008 996 8
$P_{i,j}$	9,805e-26	1,146 84e-13	0,134 140 06
Q_j	1,008 996 8	1,008 996 8	1,008 996 8
$Z_{i,j}$	2,0	1,999 999	1,0
$\frac{v_{re}}{v_{inc}}$	0,073 471 5	0,073 471 5	0,073 471 5
$C_{D,i,j}$	2,148 218 46	1,492 049	0,075 680 4
$C_{L,i,j}$	0	0,077 835 82	0,013 924 5

The C_{D} and C_{L} profiles associated with this test case, as reported by Doornbos (see Reference [39]), are shown in the Figure 23. Note that the constituent data in the example above matches the Doornbos C_{D} and C_{L} values for oxygen.

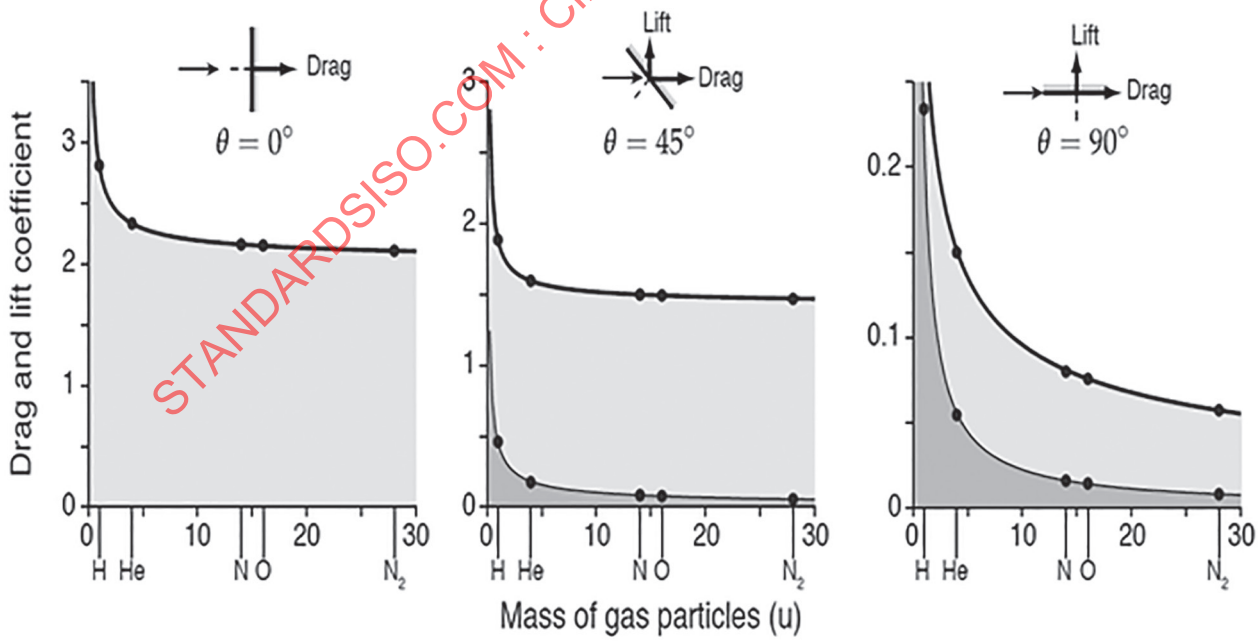

Figure 23 — Variation of drag and lift coefficients for one-sided panel as function of gas constituent

Another viable approach to drag coefficient modelling is to establish a reference $Cd = f$ (altitude) law comprised of a mean cross sectional area (Cd_{mean}) hypothesis (see Reference [28]). It is based on the value of the drag coefficient of a plate in tumbling mode.

Higher-fidelity approaches to drag coefficient estimation are also found in literature (see Reference [39]). Note that more accurate aerodynamic and radiation pressure coefficient estimation techniques do exist based upon detailed 3D geometry models with an arbitrary number of precisely positioned and shaped panels. For example, specialized software such as ANGARA (Fritsche et al., 1998) is based on CAD drawings of the spacecraft. ANGARA is able to calculate both radiation pressure and aerodynamic force coefficients using the same tools for building the spacecraft geometry. Similar techniques and software implementations are described in Ziebart (2004) and Ziebart et al. (2005) for radiation pressure effects and in Fuller and Tolson (2009) for aerodynamics.

7.3 Estimating cross-sectional area with tumbling and stabilization modes

Ballistic coefficient can have a large influence on orbit lifetime. Cross-sectional area is one of three key components (the others being mass and drag coefficient) which comprise the ballistic coefficient. In this subclause, we examine how average cross-sectional area should be estimated if not already incorporated into the drag coefficient (as was shown in the previous subclause).

If the simple panel model described above or a more sophisticated drag coefficient estimation technique is employed to estimate drag coefficient corresponding to a fixed reference area, then the ballistic coefficient shall be based on that estimated drag coefficient and its corresponding (fixed) reference area. Conversely, if a static drag coefficient is adopted, then any cross-sectional area variations shall be sampled across all expected attitudes to estimate an average cross-sectional area for incorporation into the ballistic coefficient.

If the attitude of the spacecraft cannot be anticipated (as is typically the case), the user shall compute a mean cross-sectional area assuming that the attitude of the spacecraft may vary uniformly (relatively to the velocity direction), i.e. that all the possible attitudes may be achieved with the same probability and during the same time. The mean cross-sectional area is obtained by integrating the cross-sectional area across a uniform distribution of attitude of the spacecraft (as if an observer would observe a spacecraft from any direction and compute the resulting mean observed cross-section).

In the absence of a more detailed model, a composite flat-plate model may be utilized. For example, for a plane sheet of which S is the area, it can be demonstrated that the “mean surface area” is S/2 when averaged over all possible viewing angles; by extension, for a parallelepiped-shaped spacecraft, S1, S2, S3 being the three surfaces (their opposite sides are to be neglected because when a side is visible, the opposite one is masked), it can be demonstrated that this “mean surface area” is (S1+S2+S3)/2; if a solar array of surface S4 is added, the mean surface area is then (S1+S2+S3+S4)/2 (neglecting any possible masking between the solar array and the spacecraft). This flat plate model has been shown to be accurate to within 20 % for tracked objects. Since masking effects represent a systematic bias that has the effect of reducing drag (thereby increasing orbit lifetime), an appropriately conservative cross-sectional area masking reduction factor shall be introduced to maintain accuracy.

To eliminate the need for such conservatism, this plate model approach can be extensively refined by integrating the cross-sectional area of the spacecraft across all anticipated tumbling attitudes (e.g. using a computer-aided design or CAD program), and then dividing the result by the difference between the limits of integration. The analyst is then left with a properly weighted average cross-sectional area.

For spacecraft with a large length to diameter ratio, the analyst shall consider whether gravity gradient stabilization will occur and adjust the cross-sectional area based upon the anticipated stabilized geometry. Similarly, for spacecraft which has a large aero-torque moment (i.e. the center-of-gravity and center-of-pressure are suitably far apart and the aerodynamic force is suitably large), the analyst shall consider whether the spacecraft would experience drag-induced passive attitude stabilization and adjust the cross-sectional area accordingly.

7.4 Estimating mass

The mass of the spacecraft shall be assumed to be its total mass at mission completion, where total mass is comprised of the spacecraft's dry mass plus the anticipated fuel margin of safety upon completion of the spacecraft's deorbit or safing manoeuvres. Note that such fuel margin/mass can be neglected if venting is planned prior to end of the deorbit phase (e.g. for an upper-stage).

Annex A
(informative)

Space population distribution

The launch vehicle and its family of deployed objects pass through various orbit regimes during the ascent phase from launch up to the mission orbit. As can be seen in Figures A.1 through A.4, the collision risk is especially high in specific orbital regimes (the LEO and GEO belts and at the altitudes of deployed constellations).

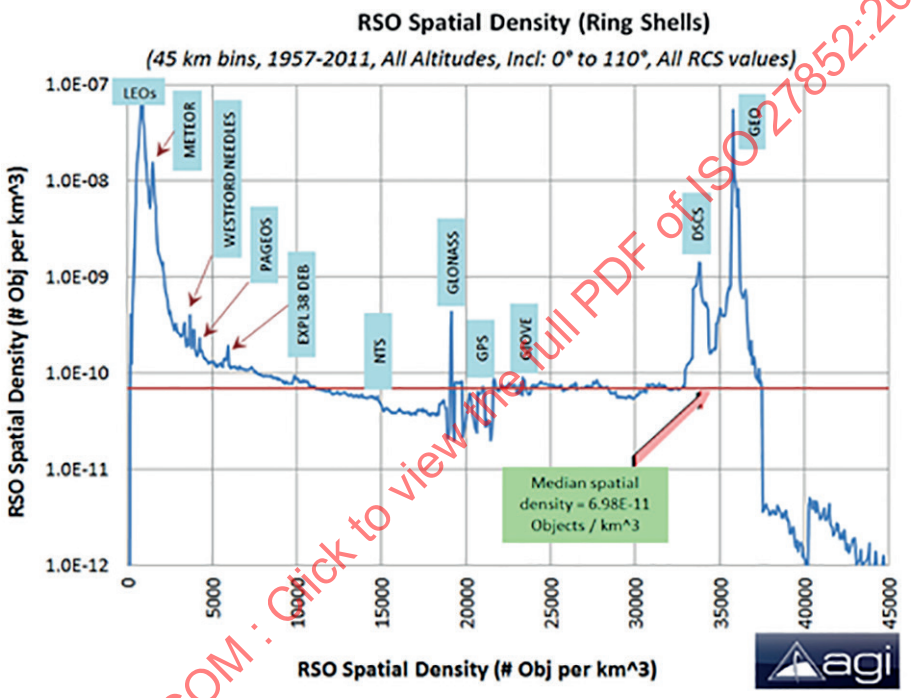

Figure A.1 — Sample near-earth space spatial density, 2011

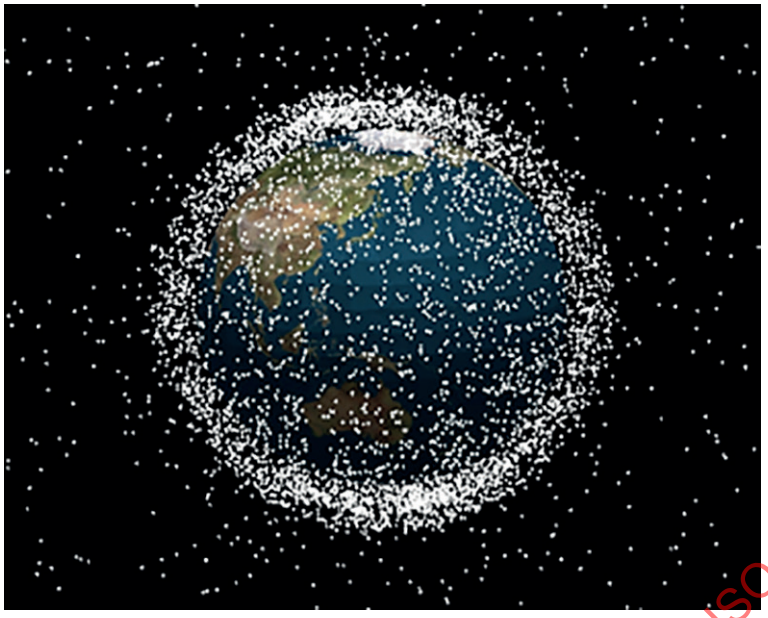

Figure A.2 — Distribution in low-earth orbit

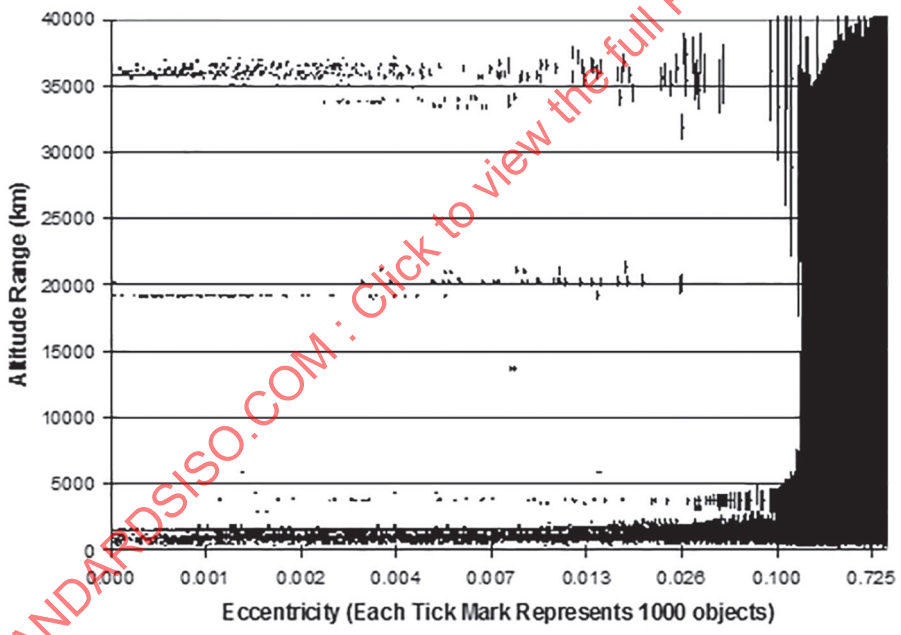

Figure A.3 — Space population by altitude and eccentricity

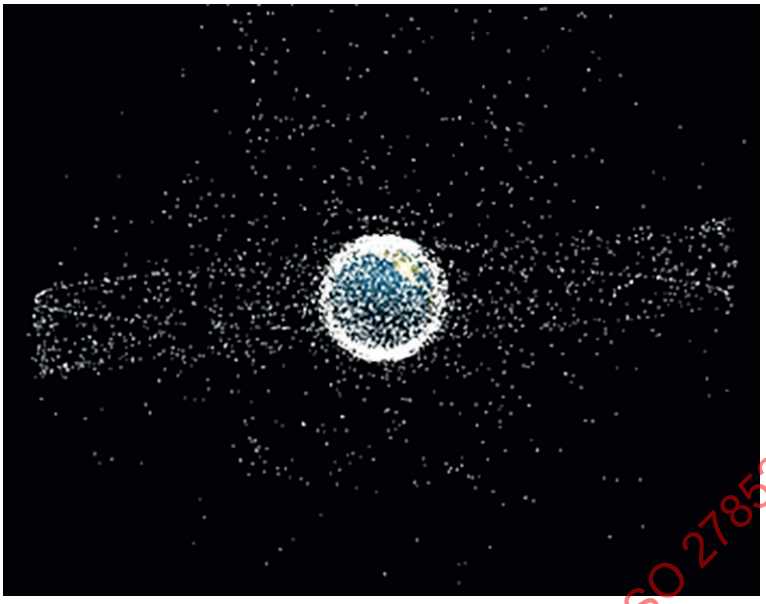

Figure A.4 — Distribution in near-earth space

Annex B
(informative)

25-year lifetime predictions using random draw approach

If the user of this International Standard wishes to estimate whether a space object has a 25-year orbit lifetime or not, a set of Method 3 analysis products have been generated and are available in this Annex. This Method 3 data were generating utilizing solar/geomagnetic modelling Approach #1, coupled with a Method 2 orbit lifetime analysis tool (1Earth research semi-analytic orbit propagator 'QPROP'). QPROP was used to examine the 8 000 000 cases contained in Table B.1, spanning a variety of times-into-the-solar-cycle, inclinations, perigee altitudes (H_p), apogee altitudes (H_a), and ballistic coefficients. QPROP uses semi-analytic propagation of mean orbit elements coupled with gravity zonals J_2 and J_3 and selected atmosphere models (including NRLMSISE-00, Jacchia-Bowman, Jacchia 1971, etc.). QPROP has been used to analyse orbit lifetime and spacecraft re-entry by several government and industrial organizations. Its accuracy has been validated by high-precision numerical integration results (Method 1 type).

Table B.1 — QPROP grid of test cases

Parameter	Lower limit	Upper limit	Step size
Time into solar cycle (days)	0	2 964,75	3 953/4
Inclination (deg)	0	90	30
C_DA/m (cm^2/kg)	25	500	25
Perigee altitude (km)	100	2 000	50
Apogee altitude (km)	250	10 000	50
Number of trials	0	3	1

The primary independent variables of the orbit lifetime estimation process are contained in Table B.1. By stepping through all of these variables in the ranges and step sizes indicated in Table B.1, and then detecting those cases which resulted in a 25-year orbit lifetime, the dependencies between ballistic coefficient and orbit initial condition can be found. While both the NRLMSISE-00 and Jacchia-Bowman atmosphere models are implemented in QPROP, the NRLMSISE-00 model was used for these analyses due to its faster runtime with similar long-term propagation accuracy. Random draws of the triad of solar and geomagnetic index parameters (discussed in 5.3) were implemented. In order to capture variations exhibited by the random draw process, a number of trials were used (four, in this case).

For a spacecraft having a ballistic coefficient of 200 cm^2/kg and starting in a circular, equatorial orbit at the altitude shown, Figure B.1 depicts the resultant ranges of anticipated orbit lifetime. The "minimum" and "maximum" incorporate the entire range of orbit decay start times with respect to the solar cycle minimum. The right-hand side of the plot shows how variable the results can get in the neighbourhood of 25-year estimated lifetime.

The dependence of orbit lifetime upon orbit inclination is shown for the same 200 cm^2/kg sample case in Figure B.2. In Figure B.2, it is seen that polar orbits experience reduced atmospheric drag, likely due to both the reduced time spent flying near the solar sub-point in combination with the reduced atmospheric density at the earth's poles due to the oblate shape of the earth and atmosphere.

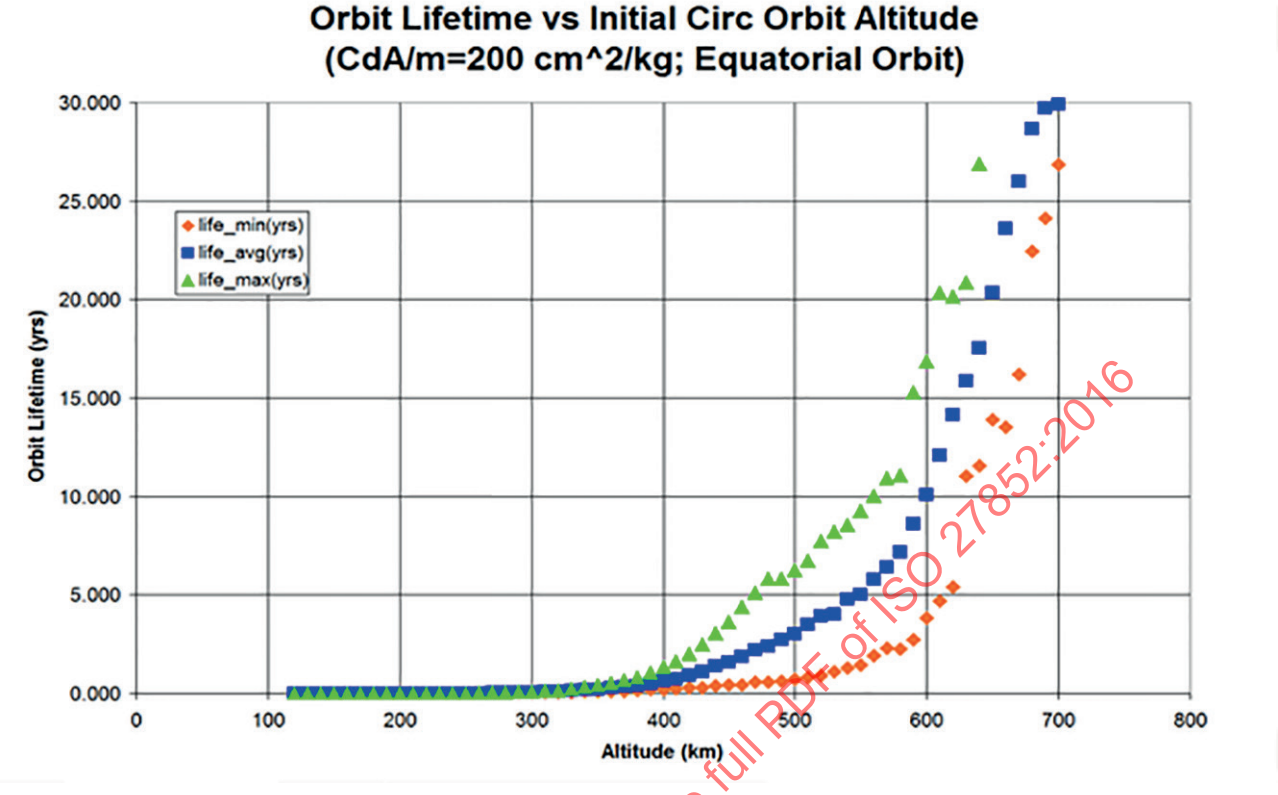

Figure B.1 — Sample orbit lifetime ($C_D A/m$ = 200 cm²/kg, equatorial orbit) as a function of initial orbit altitude

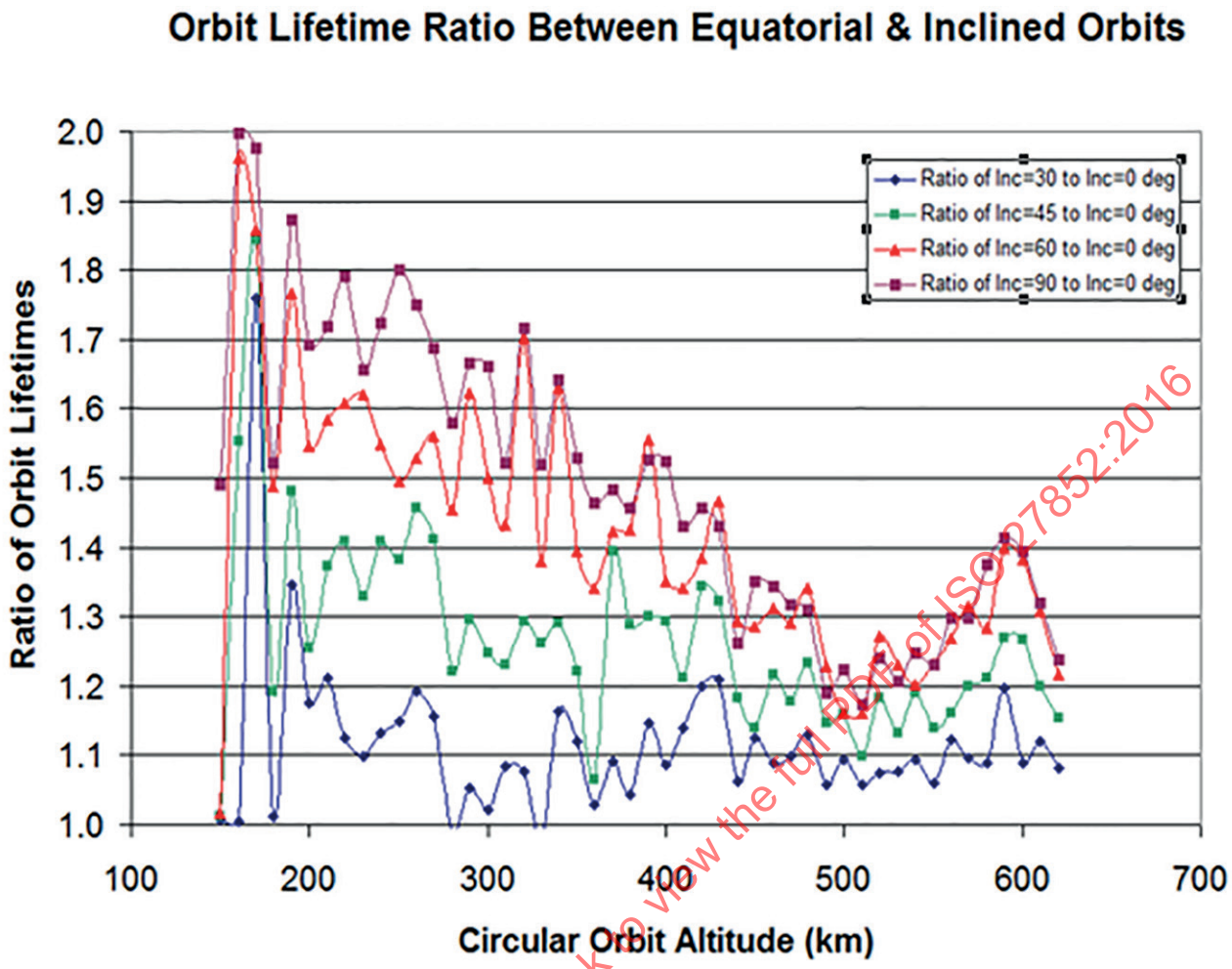

Figure B.2 — Orbit lifetime dependence upon orbit inclination

Future studies may use more trials and incorporate finer step sizes but the large computer runtime requirements of these many cases led to the initial selection of four trials per initial set of orbit conditions. Through extensive simulation, it was found for non-sun-synchronous orbits that orbit lifetime results are not sensitive to the three angular orbit elements (RAAN, argument of perigee and mean anomaly) and therefore the three initial values are arbitrarily chosen and assumed for all cases. Note that the sensitivity to RAAN and argument of perigee may be significant for sun-synchronous and more generally for high-eccentricity orbits; this was discussed in 5.5 and 5.6.

It is recommended that sun-synchronous orbit cases be studied using a "Method 1" or "2" approach until such time as their orbit lifetimes can be appropriately categorized in graphical and/or functional form. Further, it was found that orbits having inclinations greater than 90° could be well-represented by the pole-symmetric orbits having complementary orbit inclinations (justifying analysis of only 0° to 90° as shown in Table B.1).

The coloured regions shown in Figures B.3 and B.4 denote the categorization of the orbit initial conditions at the start of the orbit decay with respect to the 25-year post-mission lifetime constraint specified in ISO 24113. The "green" region denotes orbit initial conditions which will result in an orbit lifetime shorter than 25 years (in all observed cases). The "yellow" region denotes initial orbit conditions that could result in an orbit lifetime that is greater than the recommended 25-year limit, in certain circumstances.

One can observe from Figures B.3 and B.4 that there are a wide variety of initial orbit, timing, solar and geomagnetic conditions which can combine to produce an orbit lifetime of 25 years. These figures, while helpful, still leave the user with uncertain knowledge of what the post-mission orbit lifetime will